NPS67-84-005

NAVAL POSTGRADUATE SCHOOL

Monterey, California

APPLICATION OF FINITE ELEMENT CODE Q3DFLO-81
TO TURBOMACHINERY FLOW FIELDS

H. D. SCHULZ

F. NEUHOFF

CH. HIRSCH

R. P. SHREEVE

SEPTEMBER 1984

Interim Report for Period 1 October 1983-September 1984

Approved for public release, distribution unlimited

Prepared for:
Naval Air Systems Command
Washington DC 20361

NAVAL POSTGRADUATE SCHOOL
Monterey, California

Rear Admiral R. H. Shumaker
Superintendent

D. A. Schrady
Provost

The work in this report results directly from the appointment of Dr. Ir. Charles Hirsch, who is Professor and Head of the Department of Fluid Mechanics at Vrije Universiteit, Brussel, Belgium, as the Naval Air Systems Command Visiting Research Professor in Aeronautics during FY84. This appointment, under the cognizance of Dr. G. Heiche (Air 03D), was funded by the Naval Air Systems Command Air-Breathing Propulsion Research Program.

Professor Hirsch read his finite element computer program Q3DFLO-81 into the NPS IBM 370 system and subsequently instructed Turbopropulsion Laboratory students and researchers in its use.

The results herein are collected from applications of the code in several independent, but technically related, research programs. In particular, a program to examine controlled-diffusion blading designs for compressor cascades is acknowledged. Support for this exploratory development program was provided by Naval Air Systems Command under the cognizance of G. Derderian (AIR310E).

Appreciation is expressed to Professor Hirsch for the use of his code and for his contributions to the research programs.

This report was prepared by:

REPORT DOCUMENTATION PAGE

1a. REPORT SECURITY CLASSIFICATION: UNCLASSIFIED

1b RESTRICTIVE MARKINGS:

SECURITY CLASSIFICATION AUTHORITY:

3 DISTRIBUTION / AVAILABILITY OF REPORT: Approved for Public Release; distrubution is unlimited.

2b. DECLASSIFICATION / DOWNGRADING SCHEDULE:

4 PERFORMING ORGANIZATION REPORT NUMBER(S): NPS67-84-005

5 MONITORING ORGANIZATION REPORT NUMBER(S):

6a. NAME OF PERFORMING ORGANIZATION: Turbopropulsion Laboratory, Naval Postgraduate School

6b OFFICE SYMBOL (If applicable): 67Sf

7a. NAME OF MONITORING ORGANIZATION:

6c. ADDRESS (City, State, and ZIP Code): Monterey, CA 93943-5100

7b ADDRESS (City, State, and ZIP Code):

8a. NAME OF FUNDING / SPONSORING ORGANIZATION: Naval Air Systems Command

8b OFFICE SYMBOL (If applicable): AIR310E

9 PROCUREMENT INSTRUMENT IDENTIFICATION NUMBER: N0001984WR 41099, N0001984WR 41134

8c. ADDRESS (City, State, and ZIP Code): Washington, DC 20361

10 SOURCE OF FUNDING NUMBERS

PROGRAM ELEMENT NO	PROJECT NO	TASK NO	WORK UNIT ACCESSION NO
WR024	03	001	

11 TITLE (Include Security Classification): APPLICATION OF FINITE ELEMENT CODE Q3DFLO-81 TO TURBOMACHINERY FLOW FIELDS (UNCLASSIFIED)

12 PERSONAL AUTHOR(S): H. D. SCHULZ, F. NEUHOFF, CH. HIRSCH and R. P. SHREEVE

13 TYPE OF REPORT	13b TIME COVERED	14 DATE OF REPORT (Year, Month, Day)	15 PAGE COUNT
Interim	FROM SEP 83 TO SEP 84	September 1984	53

16 SUPPLEMENTARY NOTATION:

17 COSATI CODES			18 SUBJECT TERMS (Continue on reverse if necessary and identify by block number)
FIELD	GROUP	SUB-GROUP	Finite Element Code Turbomachinery Flow Fields Through-Flow Calculations

19 ABSTRACT (Continue on reverse if necessary and identify by block number)

Through-flow and blade-to-blade calculations were made in association with a number of experimental research activities at the Turbopropulsion Laboratory, Naval Postgraduate School. The Q3DFLO-81 code was operated on an IBM 370-3033 mainframe computer. The flow through a single stage axial research compressor was computed and compared with both probe survey and stage performance map measurments. Swirling flow produced by a vaned out-flow generator for a radial diffuser test facility was calculated for both large low-speed and small-scale high-speed versions of the device. Flow through a two-dimensional compressor cascade of "controlled-diffusion" blade shapes was calculated and the results compared with experimental data, and with predictions obtained using the NASA code QSONIC.

20 DISTRIBUTION / AVAILABILITY OF ABSTRACT: ☒ UNCLASSIFIED/UNLIMITED ☐ SAME AS RPT ☐ DTIC USERS

21. ABSTRACT SECURITY CLASSIFICATION: UNCLASSIFIED

22a NAME OF RESPONSIBLE INDIVIDUAL: R. P. SHREEVE

22b TELEPHONE (Include Area Code): (408)646-2593

22c OFFICE SYMBOL: 67Sf

DD FORM 1473, 84 MAR — 83 APR edition may be used until exhausted. All other editions are obsolete.

ABSTRACT

Through-flow and blade-to-blade calculations were made in association with a number of experimental research activities at the Turbopropulsion Laboratory, Naval Postgraduate School. The Q3DFLO-81 code was operated on an IBM 370-3033 mainframe computer. The flow through a single stage transonic axial research compressor was computed and compared with both probe survey and stage performance map measurements. Swirling flow produced by a vaned out-flow generator for a radial diffuser test facility was calculated for both large low-speed and small-scale high-speed versions of the device. Flow through a two-dimensional compressor cascade of "controlled-diffusion" blade shapes was calculated and the results compared with experimental data, and with predictions obtained using the NASA code QSONIC.

TABLE OF CONTENTS

LIST OF FIGURES

LIST OF TABLES

I. INTRODUCTION

Attempts to model the complex three-dimensional flow in turbomachines have resulted in the development of various quasi three-dimensional numerical techniques.

Most methods follow the work of Wu (Ref. 1), wherein the fully 3D flow is resolved into a succession of 2D-calculations. The flow is solved on meridional surfaces (S2), and blade to blade surfaces (S1). In general, the intersection of an S1 surface and an S2 surface is a twisting line with three dimensional variations. The interaction of the two families of surfaces can be quite complicated. However, if an axisymmetric assumption is made, the S2 surfaces will become identical to the meridional plane. An important drawback in this method is the lack of knowledge on the degree of approximation which is made by assuming axisymmetry.

The program used in the present study, therefore, follows another approach where the S2-surface calculation is replaced by the calculation of the flow in the true meridional section (R-2 plane), based on the solution of exact pitch averaged equations. The numerical method used to solve the equations in the meridional and blade to blade plane is the finite element method. An interconnection of the meshes allows for a consistent interaction to be defined in the calculation.

Q3DFLO-81 is only valid in the absence of backflow and hence does not handle separation regions or secondary flow. The calculations are based on the existence of an inviscid core flow, but accommodates empirical input with regard to loss levels, slip factors and axial-velocity-density ratio (AVDR), or superimposes a two dimensional boundary layer calculation. The program is

described in References 2 and 3. The procedure to run the code on the Naval Postgraduate School (NPS) computer is given in Reference 4. The present report describes the application of this code to various turbomachinery flow fields. Results from applying the through-flow calculation to a transonic axial compressor and to a novel radial cascade are given in Section 2. In Section 3 results from the blade to blade calculations applied to a controlled diffusion compressor stator section are compared with measurements taken in a linear cascade and with the results from the finite difference code QSONIC. The conclusions drawn from these applications are given in Section 4.

II. THROUGH FLOW CALCULATION

A. Axial Compressor

A single stage, small diameter (11 inches) high speed axial flow compressor, of in house design, was investigated (Fig. 1). Test data from radial surveys at different axial locations and overall machine performance at various stage conditions were compared with results of corresponding computer runs. Furthermore, a compressor performance map for machine speeds higher than those already tested was calculated to estimate the machine conditions at higher speeds. Figure 2 shows the calculation mesh for the compressor. Thirteen streamlines run from three rotor tip chord lengths upstream of the rotor leading edge to about 2 rotor tip chord lengths downstream of the rotor trailing edge. Station lines 5, 8 and 13 are placed axially in a way that they coincide with probe traverse locations. The rotor leading edge corresponds to station 9, trailing edge to station 12, and the stator leading edge is located at station 15, with its trailing edge at station 18. Rotor and stator geometry input is limited to blade inlet and outlet angles, maximum relative blade thickness, solidity, chord length and leading edge radius. These quantities have to be given for a number of blade cuts at different radii. They must also be parallel to the centerline. This made a recalculation of the blade profile coordinates necessary, since in the original design they were specified on conical surfaces. The cross-section of stage inlet and outlet up and downstream of the regime shown in Fig. 2 is constant and cylindrical. A small fillet at the tip of the rotor spinner was incorporated in the geometry input to eliminate the blunt stagnation point singular condition. Using the mesh shown in Fig. 2, calculations were performed in which input quantities (besides the geometry) were taken from a

compressor test run. This test run provided results from three radial surveys at locations corresponding to calculation stations 5, 8 and 13. These stations serve to evaluate flow into and out of the rotor. Stator outlet measurements were not available. Figures 3 through 16 show comparisons of measured and calculated radial distributions. In Fig. 3 fair to good agreement is shown for the absolute flow angle. The axial velocity component (Fig. 4) does not agree too well for the lower portion (40%) of the channel height at station 5. The change in geometry used in the calculation is probably the cause for this variation.

In the following figures, comparisons are shown only for calculation stations 8 and 13 and the corresponding test results, since the main purpose of the investigation was to evaluate the compressor rotor. The radial velocity component (Fig. 5) seems to have rather large discrepencies for station 8 (rotor inlet), especially in the hub region. If, however, the radial velocity component is converted to flow pitch angle, the difference shown represents an error of no more than four degrees. In Fig. 6 the absolute flow Mach number for rotor inlet and outlet are compared. The discrepencies in the tip areas, also apparent in Figures 3 and 4, are the result of a measurement error due to a casewall effect on the probes used. For the evaluation of the rotor performance, total pressure (Fig. 7) and total temperature (Fig. 8) at the inlet and outlet were observed. The total pressure distribution measured is constant over the blade span. A distinct increase of the outlet total temperature was calculated in the tip region. Variations in total temperature measurements are known to reflect changes in ambient conditions. Thus a temperature differential calculated between rotor inlet and outlet would not show the variations of those in Fig. 8. Further

evaluating the stage flow, Figures 9 through 11 show incidence angle, deviation angle and loss distributions, hub to tip. Again, for the rotor a comparison between measurement and calculation is given. The discrepencies in rotor incidence angle at the hub and tip are rather large while the stator shows good agreement near the tip and qualitative agreement along the span (Fig. 9). The rotor deviation angle also shows disagreement near hub and tip. The stator deviation angles predicted by the program appear to be fairly large, especially in the tip region. No test data are available for comparison, but the magnitudes used in the design of the blading were similar to those in Fig. 10. Figures 12 through 16 show distributions of other flow quantities calculated for the same axial positions.

For the compressor stage, the performance was carefully measured for the full throttle range at 60% and 70% of design speed. The program calculates the overall stage performance data. In Fig. 17, calculated and measured compressor performance are compared. The agreement in the total pressure ratio is quite good. Two efficiencies calculated by the program are shown. The total efficiency takes the casewall boundary layer and the losses associated with it into account, while the adiabatic efficiency excludes case wall effects. The discrepency between measured and calculated total efficiency is quite large and has yet to be explained.

In order to estimate the compressor performance for higher speeds, calculations were carried out for 80, 90 and 100% of design speed for a variety of flow rates. Uncertainties in the efficiency calculation were accepted. In Fig. 18, the predicted performance map is shown. It can be observed, that the efficiency curves drop off more drastically for higher flow

rates at high speeds. This is typical for high speed compressors. The calculated pressure ratio of 1.715 at 100% design speed is considerably higher than the value expected in the design process (1.5-1.6), and the referred flow rate of 19.7 lbs/sec is somewhat lower than the design value of 21.24 lbs/sec. However, this is the first attempt to predict the performance of the compressor hardware, as built, and the differences may well be explained by an error which was built in to the rotor blade setting angles (Ref 5).

B. Low Speed CDTD

A large scale subsonic radial cascade wind tunnel has been designed at the Turbopropulsion Laboratory (TPL) at NPS to investigate flow phenomena in and the performance of radial diffusers (Ref. 6). Various approaches to analyze the aerodynamic operating conditions and the flow at the test section inlet of the Centrifugal Diffuser Test Device (CDTD) have been conducted (Ref. 7).

Q3DFLO-81 accepts cylindrical inlet flow planes and was applied to the CDTD geometry. Figure 19 shows a plot of streamlines and a cross section of the axisymmetric flow channel between the inlet "swirl vane cylinder" (station 1) and diffuser-vane leading edge (station 18). The flow is introduced almost tangentially along the inlet plane at a radius of 19 inches, and then passes outward through an angular contraction to the test section inlet at a radius of 25 inches. The flow however, does not follow the physical contour of the wall (see Fig. 19) and separates in the corners between station 4 and station 6. The corner shape of the flow channel had to be approximated by a smooth contour in order for the code to operate.

Q3DFLO-81 accommodates a very versatile post processor and delivers printouts and plots of the calculated flow properties at every required flow

station. Figure 20 shows plots of spanwise distribution of axial velocity, Mach number, static pressure and flow angle for the different flow stations shown in Fig. 19.

The plots represent the inviscid solution of the core flow, considering a blockage factor determined by the end wall boundary layer calculations for hub and tip. It can be seen that the influence of the strong curvature in the contraction region (stations 7-15) has almost decayed at the test section inlet (station 18), and the flow properties are almost evenly distributed over the span. Figure 21 shows a boundary layer thickness of 20% at the test section. The boundary layer also experiences a strong acceleration in the contraction region. The velocities in the boundary layers are smaller, and more nearly tangential. Figure 22 is a comparison of predicted and measured spanwise flow angle distribution. The solid line represents the predicted flow angle for the inviscid solution as in Fig. 19. The circle indicates the calculated boundary layer thickness and the maximum angle at hub and tip. The triangles are data acquired by the first author (Ref 7). The plot shows good agreement of predicted and measured flow angles. The deviation in the mass averaged measured and calculated flow angles is only 0.5%.

C. High Speed CDTD

One of the main objectives of the low speed cascade was to examine the design concepts with a view to applying them to the design of a transonic device; the high speed CDTD.

Q3DFLO-81 is capable of calculating transonic flow in a meridional through flow calculation as long as the meridional velocity remains subsonic. A high speed cascade has been proposed with a nearly tangential Mach number of 1.48 and a total pressure of 1.6 bar at the inlet plane. The geometry of the

flow channel is qualitatively similar to that of the low speed cascade. The dimensions are smaller to reduce the massflow required to obtain higher velocities and the curvatures are reduced to avoid flow separation. Figure 23 shows the flow channel geometry which was analyzed. Station 1 is at a radius of 10 inches. Station 12 is at a radius of 12 inches.

The results obtained by applying Q3DFLO-81 to the high speed CDTD are shown in Fig 24. Shown are results for the inviscid core flow, including spanwise distributions of static pressure, Mach number, flow angle and meridional velocity. Even though the Mach number of the overall velocity was always supersonic, the meridional velocity remained subsonic. Consequently, shocks should not appear in the flow into the test section.

III. BLADE TO BLADE CALCULATION

The blade to blade calculation of the code Q3DFLO-81 is used in the quasi-3D calculation for turbomachinery blade rows as described in Section 2.1 or for isolated blade-to-blade calculations. The application to linear cascades will be described in this section.

A. NASA Controlled Diffusion Blade

A numerical optimization technique to design a controlled diffusion blade shape was developed by NASA (Ref. 8). It allows analytical design of airfoils which are shock free at transonic Mach numbers and avoids suction surface boundary layer separation for the range of inlet conditions necessary for stable compressor operation.

The on- and off- design performance of one design of such blades have been measured in a subsonic linear wind tunnel. The facility is described in detail in Ref 9 . The tests conducted with a controlled diffusion blading section designed for a compressor stator at mid-span are described in Ref. 10. Cascade configuration parameters are given in Table I. Table II presents the coordinates of the test blades.

Q3DFLO-81 was used to calculate the blade surface pressure distributions to compare with measurements. Figure 25 shows the blade shape and Fig. 26 shows a typical finite element mesh for the blade to blade calculation. In order to avoid the sharp increase in velocity, due to the potential flow effect around a thick trailing edge, the trailing edge radius was removed. The inviscid flow in fact does not see the trailing edge radius due to the viscous behavior and thus the geometry should be modeled in this way. The strong curvature at the leading edge of the blade also caused peaks in velocity, as the inviscid flow negotiates the large curvature from stagnation point to suction surface. To calculate such a leading edge shape, the mesh

has to be much finer around the leading edge than Q3DFLO-81 is able to produce (due to a restriction in the number of mesh points). The leading edge, therefore, also had to be adapted to this situation. The remainder of the flow field should be reliable since the occurance of velocity peaks seldom invalidates more than a few grid points in their vicinity. Particularly with these compressor blade geometries, the adverse pressure gradient tends to discourage the velocity variation from propagating very far or reflecting off the downstream boundaries. The influence of the flow at 5% of chord downstream of the leading edge, and 5% of chord upstream of the trailing edge is only 0.1%, therefore the calculation is accurate for 90% of the chord. Figure 27 is a plot of streamlines which shows that the flow tangency condition is very well satisfied along the blade surface and no flow separation is encountered. Figure 28 is a comparison of predicted and measured pressure coefficients along the blade surface for different inlet air angles. Very good agreement is achieved for high inlet angles (38.9°, 42.9°, 45.9°). The two smaller values at the suction side between 60% and 80% chord are errors in the measurements, probably due to plugged pressure taps. For smaller inlet air angles (24.4°, 28.0°, 32.95°) the measured values are slightly smaller than those predicted by Q3DFLO-81. The highest deviations are noticed at 32.95° incidence. Figure 29 is a plot of the measured AVDR versus inlet air angle. It is noted that the AVDR does not depend simply on the static pressure rise as is shown in Fig. 30. The AVDR in the tests reported in Ref. 10 was determined by measuring and integrating mass flux distributions at midspan upstream and downstream of the blade row. The technique is described in detail in Ref. 11. In the present calculations the AVDR was assumed to be constant from the measuring plane upstream of the blade

row to the leading edge, and from the trailing edge to the downstream measuring plane, and to have a linear distribution along the chord. The AVDR is input to Q3DFLO-81 to account for quasi-3D-effects. The assumed distribution of the AVDR along the chord of the blade might not be sufficiently representative of the experimental conditions and this could be responsible for the observed deviations.

B. Comparison with Finite Volume Code QSONIC

QSONIC is a FORTRAN computer code developed by NASA and is described in detail in Ref. 12. It is capable of calculating the flow field about a cascade of arbitrary 2-D airfoils and approximating the three-dimensional flow in turbomachinery blade row by correcting for streamtube convergence (AVDR) and radius change in the through flow direction. The program uses a conservative solution of the full potential equation combined with the finite volume method on a body-fitted periodic mesh. It is capable of calculating through weak shocks (peak relative Mach number less than 1.4) by introducing an artificial density in the transonic regions. The code has been adapted to the NPS computer (Ref. 13) and was used for comparison with Q3DFLO-81.

Q3DFLO-81 and QSONIC are both inviscid codes and solve the potential flow equations. In the Mach number range of the linear cascade (the Mach number of the flow at the inlet to the blade row is 0.25), they were expected to give basically the same results. Figure 31 compares the results of both codes with measurements from Ref. 10. They are in good agreement and show the same limitations for the calculation of the flow around the leading and trailing edges.

Even though grid generator and flow solution runs can be separated while operating QSONIC, it requires 12 minutes CPU time for the flow solution

while Q3DFLO-81 requires only eight seconds. For applications at low Mach numbers Q3DFLO-81 is much faster for the same degree of accuracy. It also provides a convenient post-processor which produces plots of mesh, blade shape and the calculated results. QSONIC should be used for Mach numbers on the blade surface from 1.0 to 1.4.

IV. CONCLUSIONS

The experience of applying the computational code Q3DFLO-81 to several turbomachinery flow problems allowed the following conclusions to be drawn:

1. Despite the apparent complexity of the geometry, the application of the code to the transonic compressor stage was straight-forward. The mesh was simple and resulted in very modest CPU times.

2. In the compressor stage analysis, the inlet flow to the rotor was very well predicted. Flow incidence angles were computed well except near the hub. Deviation angles from the rotor were within 3° of the measured values with the largest departures near hub and tip. The computed rotor losses agreed qualitatively with measured distributions but were smaller in magnitude. The stage efficiency was computed to be lower than the measured values, suggesting an inconsistency which must yet be explained.

3. Application of the code to the swirling flow generation within a centrifugal diffuser test device (CDTD) required only that minor geometrical approximations be introduced. Inlet and outlet boundary conditions were within the capability of the existing code.

4. In the low speed CDTD, the computed spanwise distribution of flow properties at the outlet did not agree with the measured values suggesting the importance of viscous effects. The mass-averaged outlet flow properties agreed quite well.

5. The code was applied with apparent success to calculate transonic swirling flow within a high-speed CDTD, and could therefore be used to design a suitable channel shape.

6. The prediction of the code in blade-to-blade calculations agreed well with measurements made in a linear subsonic cascade. Leading and trailing edges of the blades had to be modified to avoid non-physical velocity peaks, but the influences of the modifications were negligible 5% chord downstream of the leading edge and 5% chord upstream of the trailing edge.

7. Excellent agreement was obtained with the blade-to-blade predictions of NASA's code QSONIC at a test Mach number of 0.2. However, the Q3DFLO-81 code required 8 seconds of CPU time compared to 12 minutes for QSONIC.

Overall, the experience of the individual investigators was that the code could be applied successfully with limited guidance from the code's author. The post processor package was extremely valuable, and was implemented without difficulty on the NPS computer.

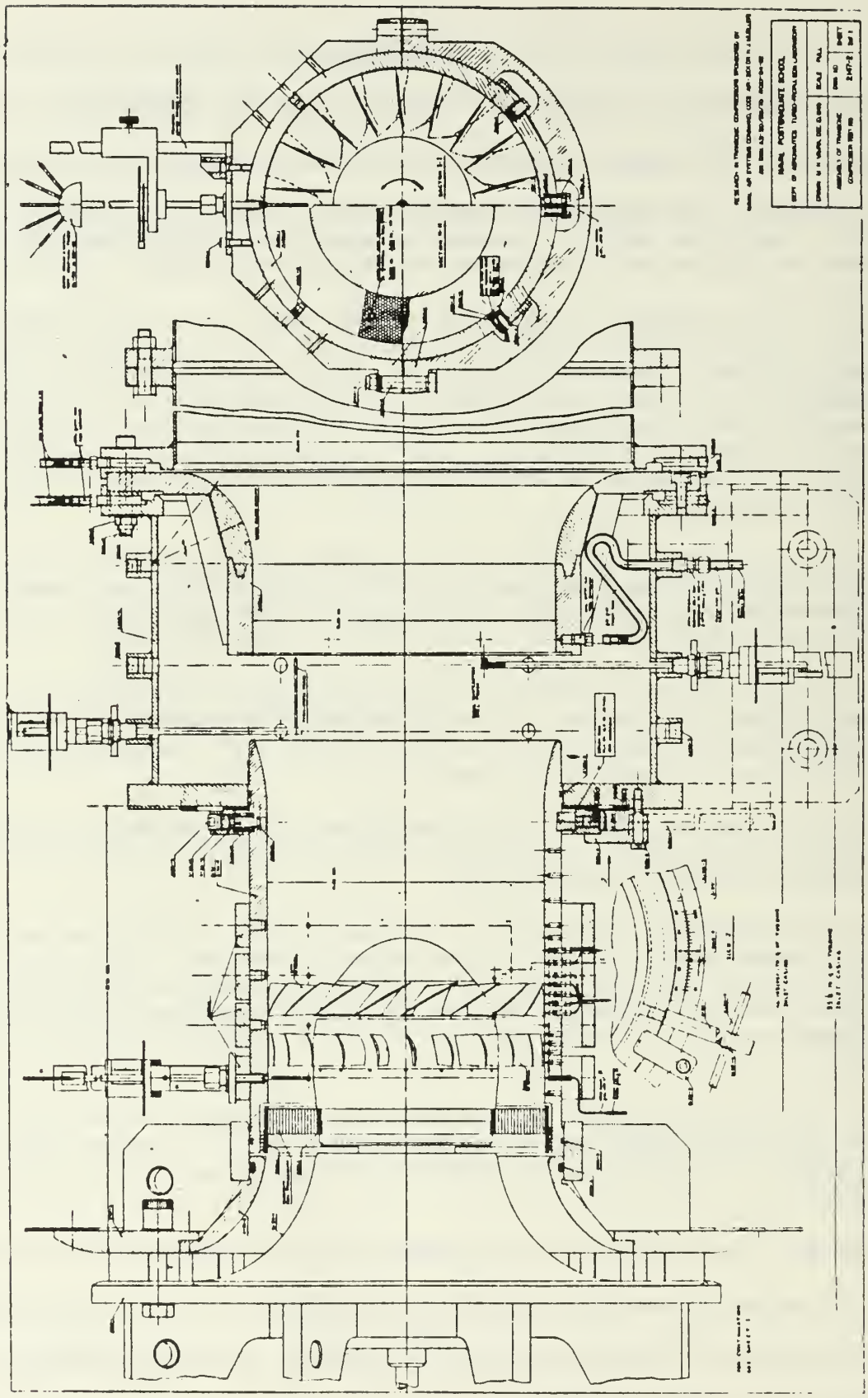

Figure 1. Transonic compressor cross-section.

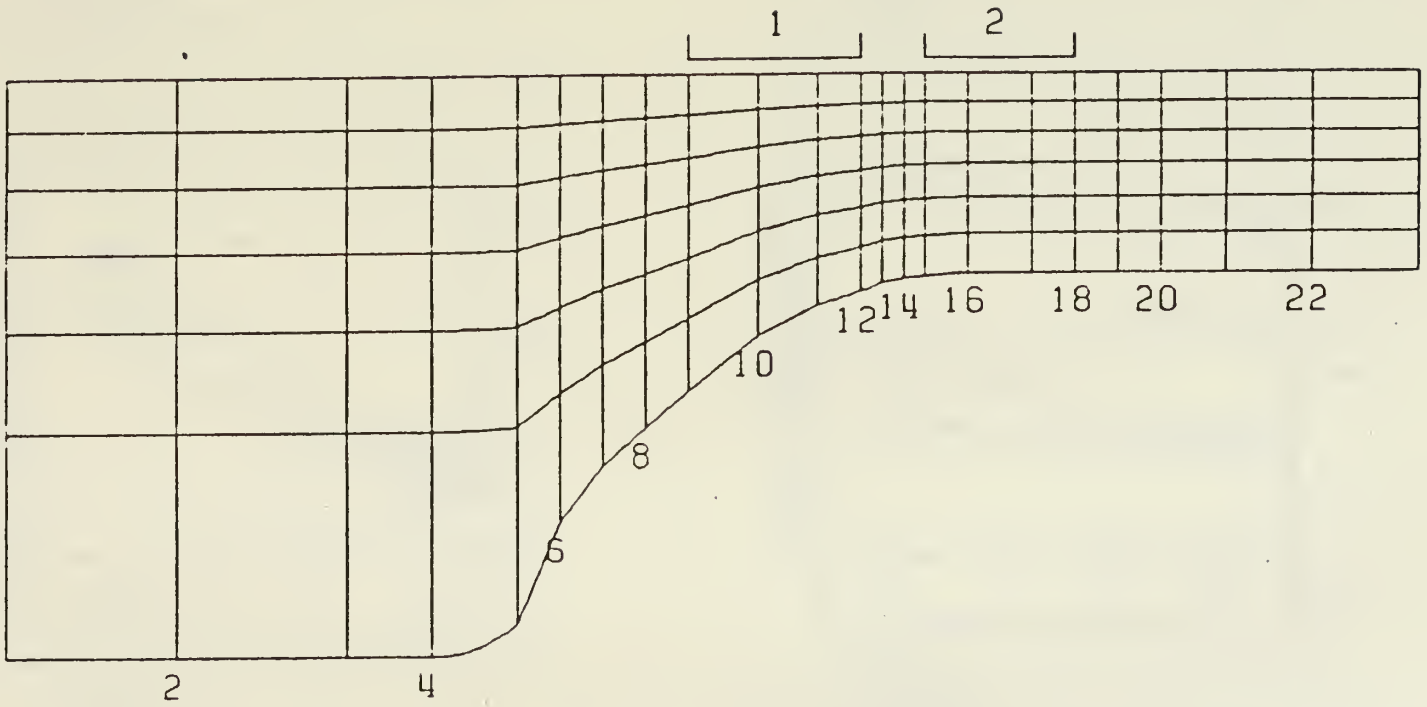

Figure 2. Compressor computational mesh

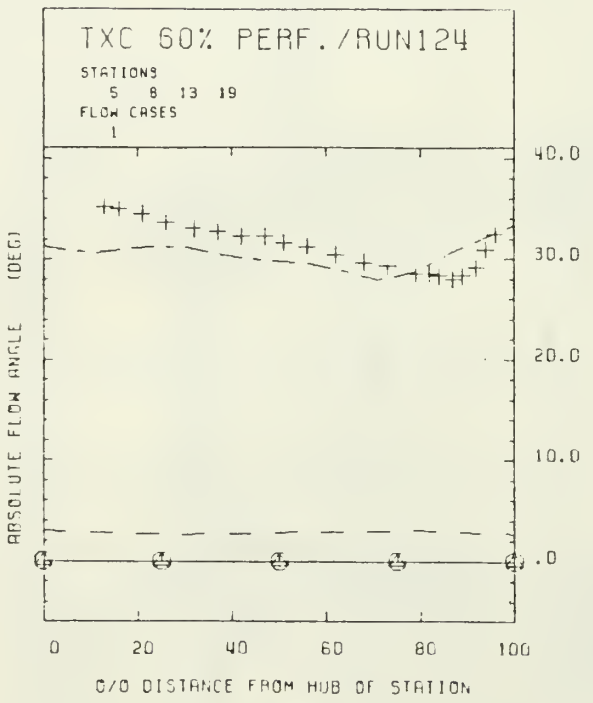

Figure 3. Absolute flow angle vs. % distance from hub.

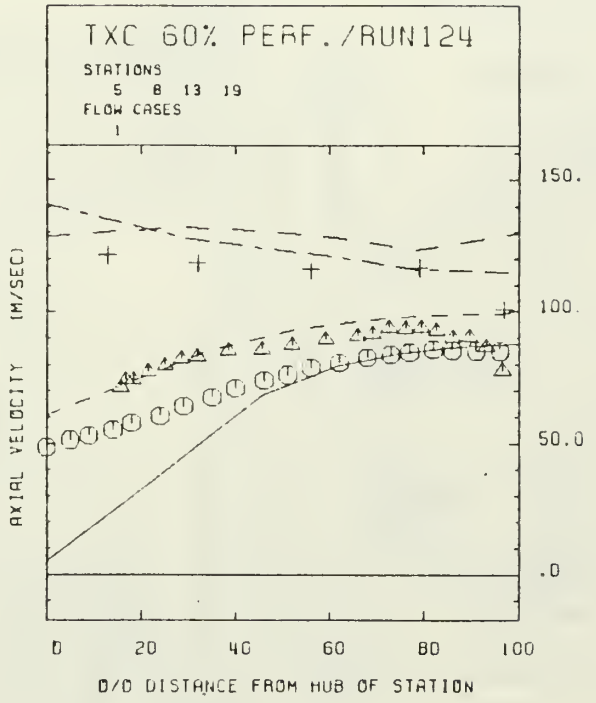

Figure 4. Axial velocity vs. % distance from hub.

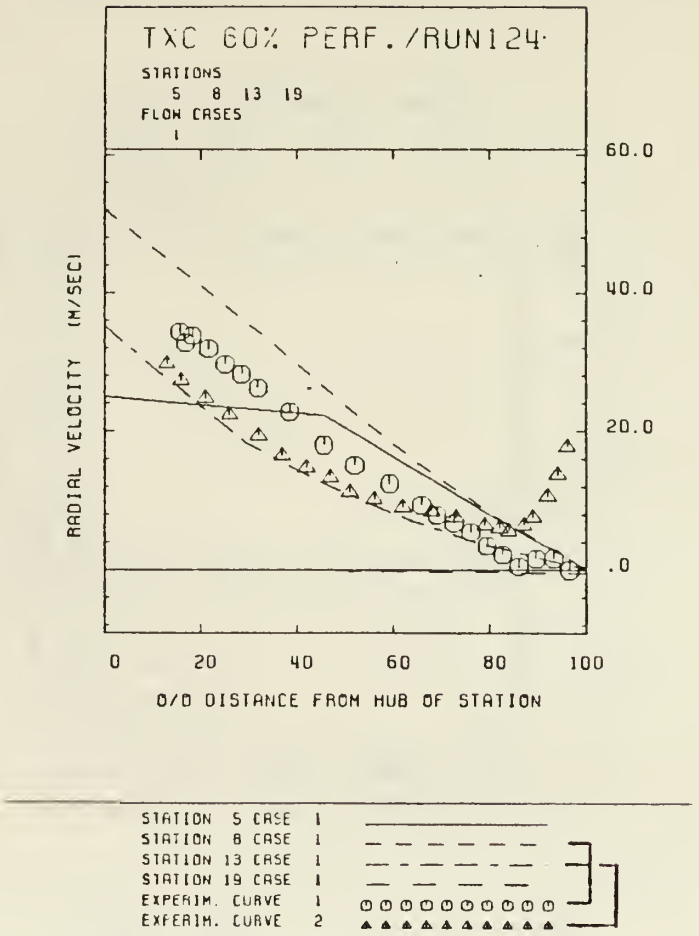

Figure 5. Radial velocity vs. % distance from hub.

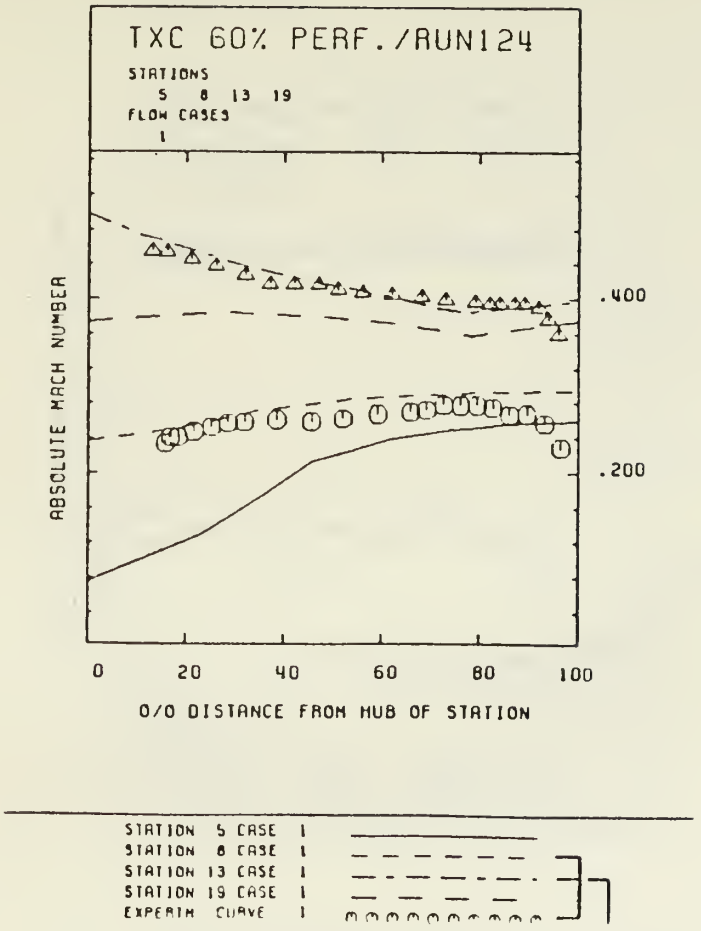

Figure 6. Absolute Mach Number vs. % distance from hub.

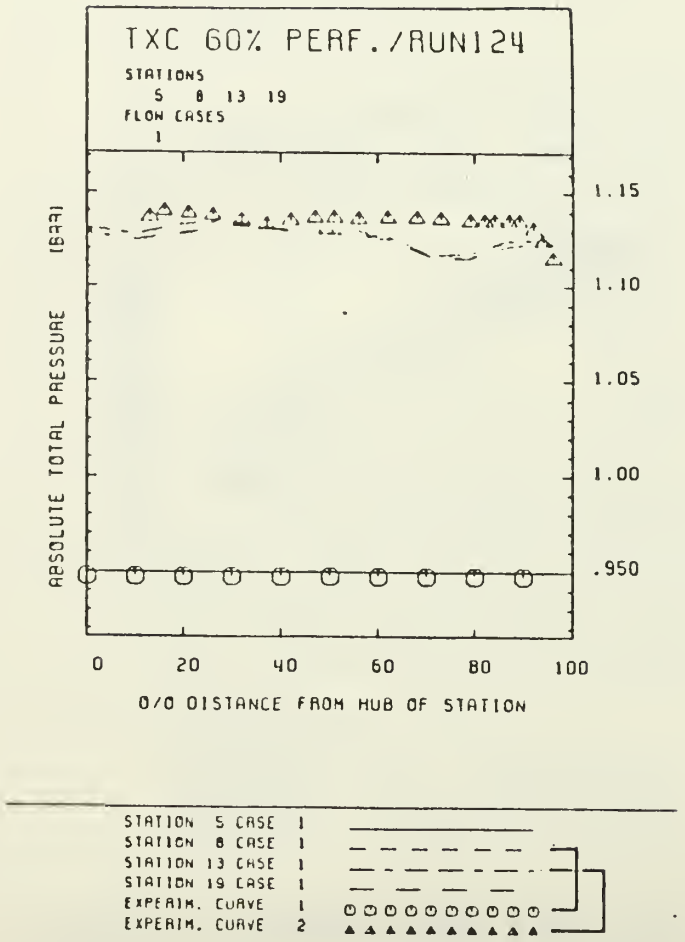

Figure 7. Absolute total pressure vs. % distance from hub.

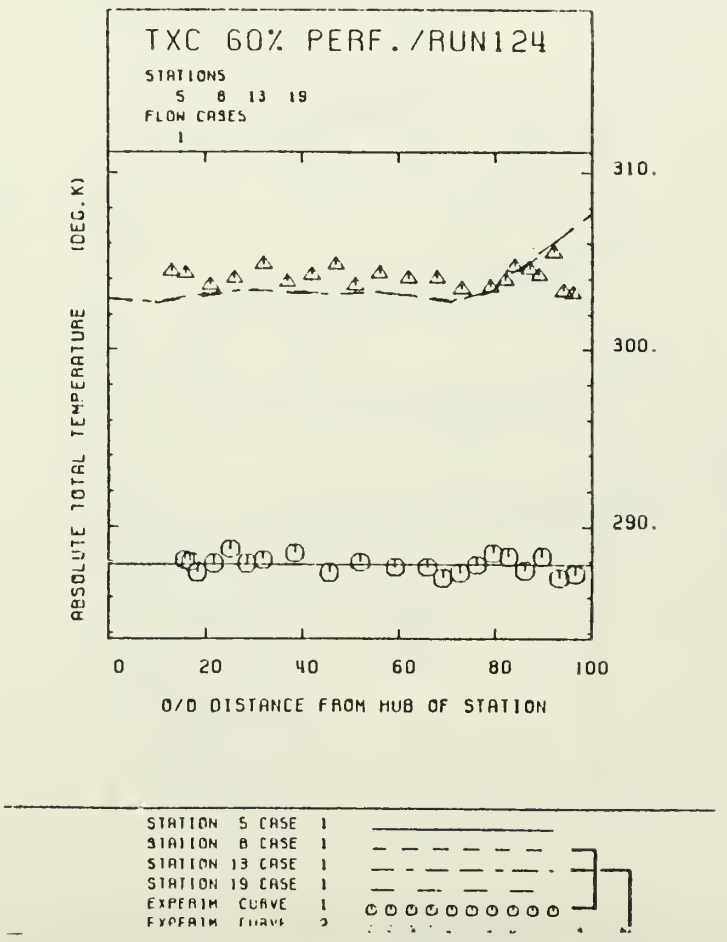

Figure 8. Absolute total temperature vs. % distance from hub.

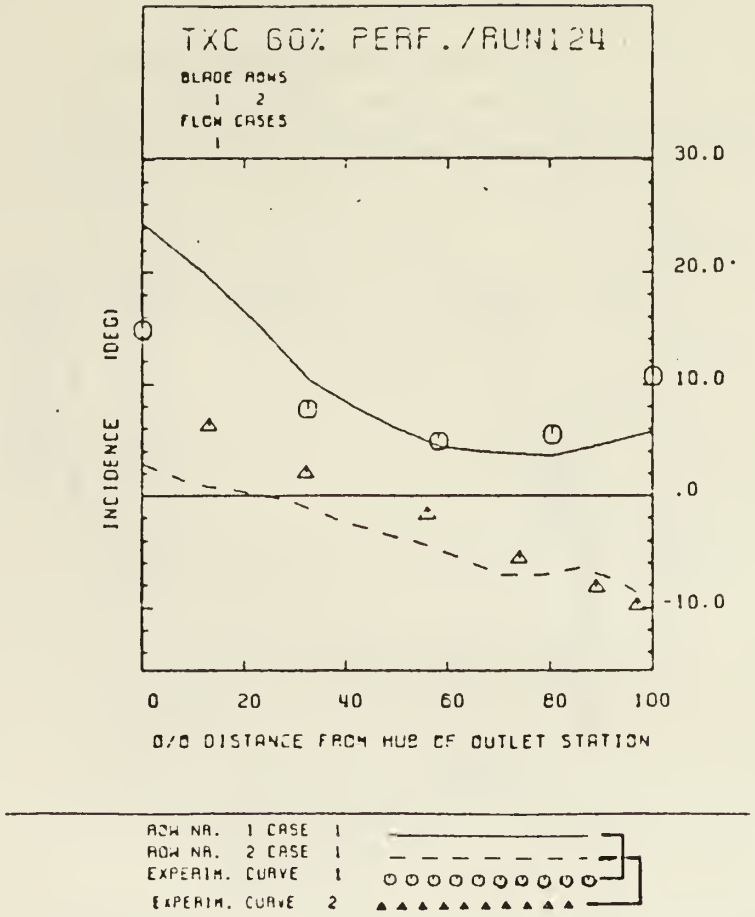

Figure 9. Incidence angle vs. % distance from hub.

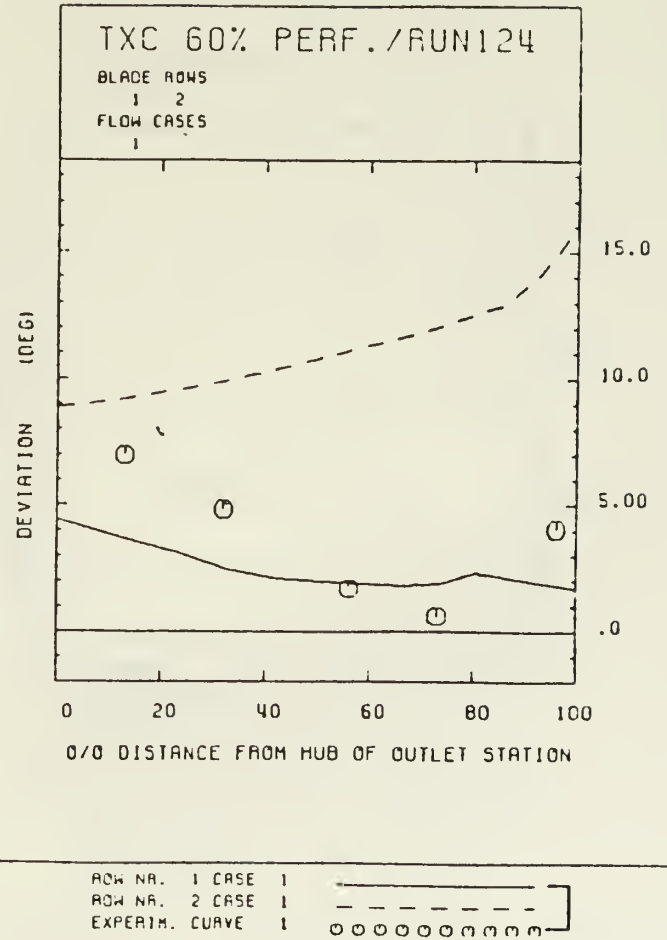

Figure 10. Deviation angle vs. % distance from hub.

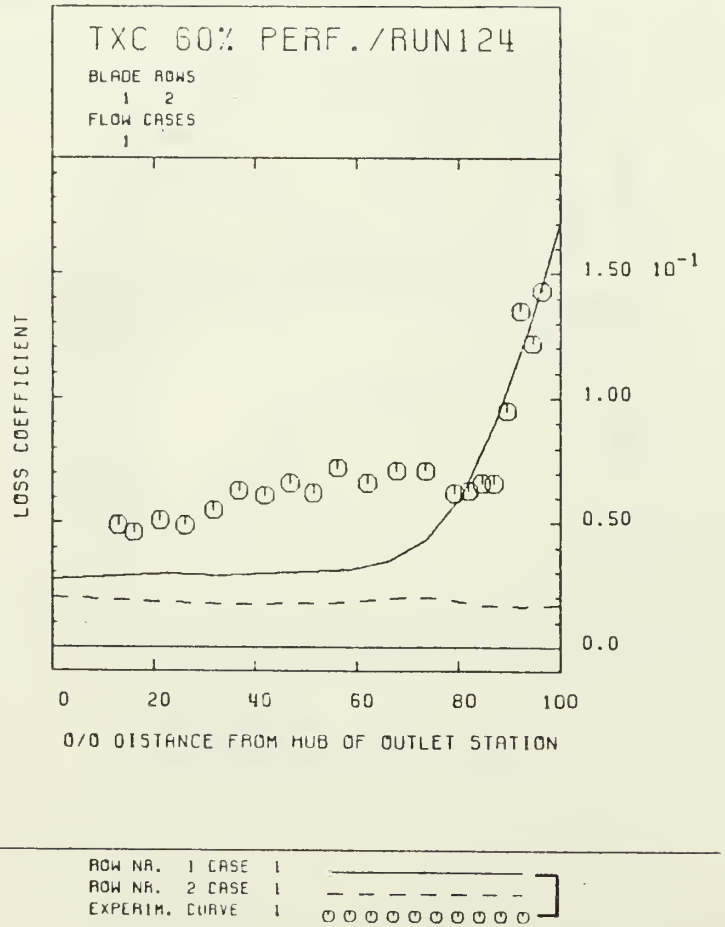

Figure 11. Loss coefficient vs. % distance from hub.

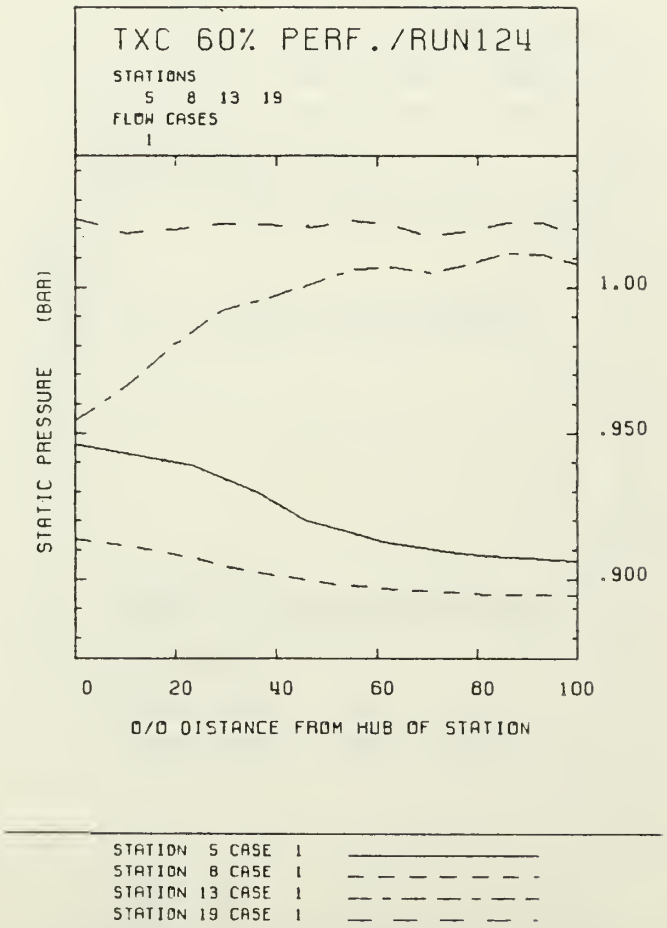

Figure 12. Static pressure vs. % distance from hub.

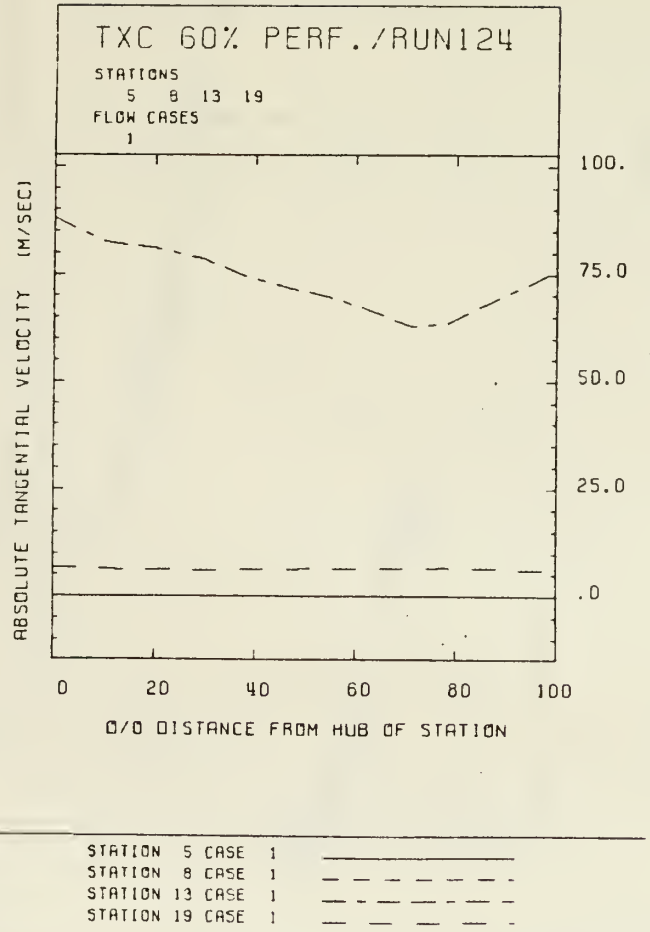

Figure 13. Absolute tangential velocity vs. % distance from hub.

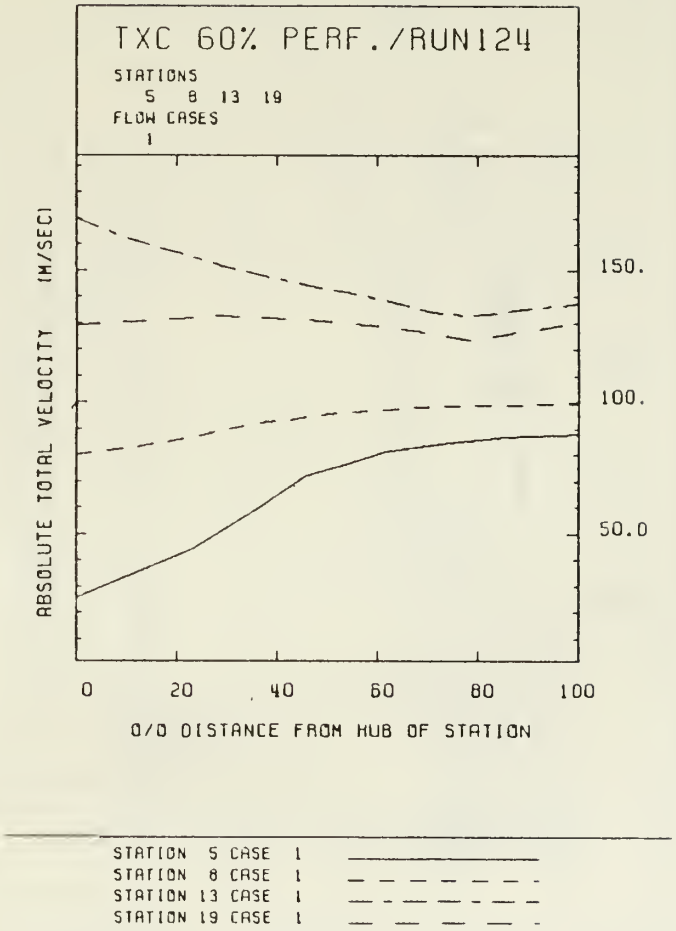

Figure 14. Absolute total velocity vs. % distance from hub.

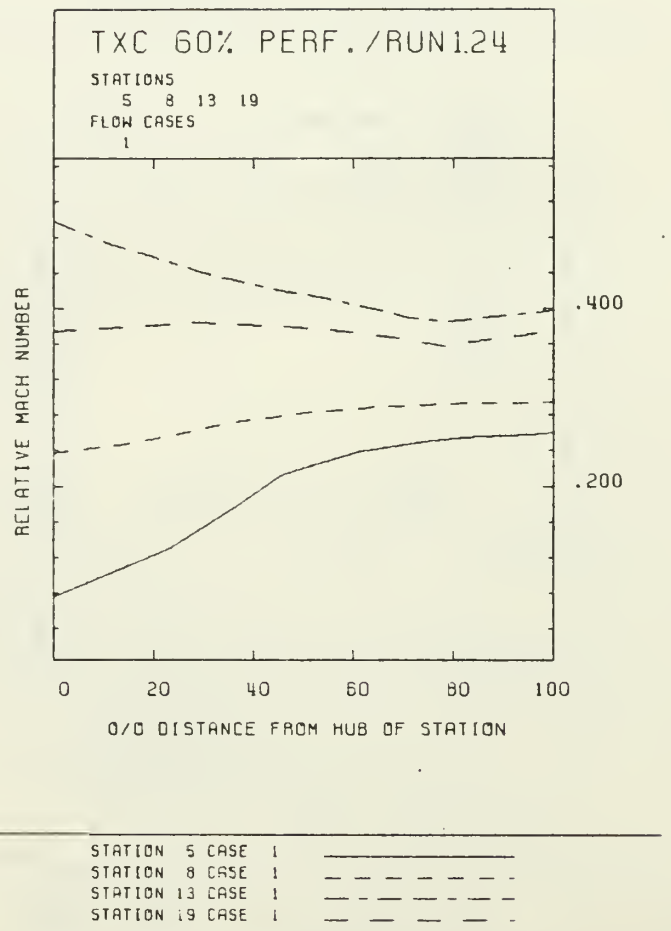

Figure 15. Relative Mach Number vs. % distance from hub.

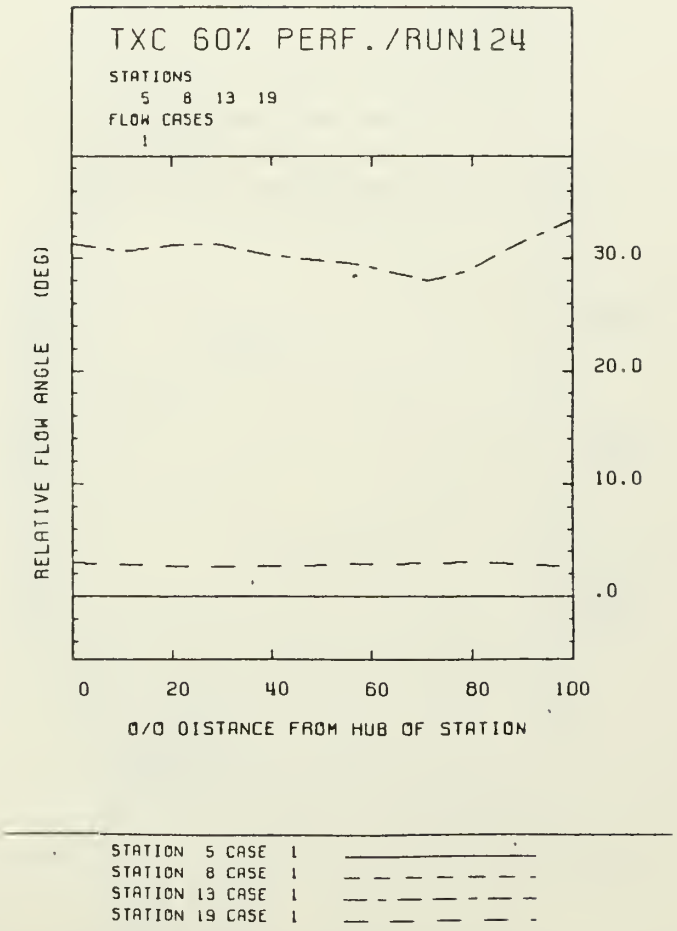

Figure 16. Relative flow angle vs. % distance from hub.

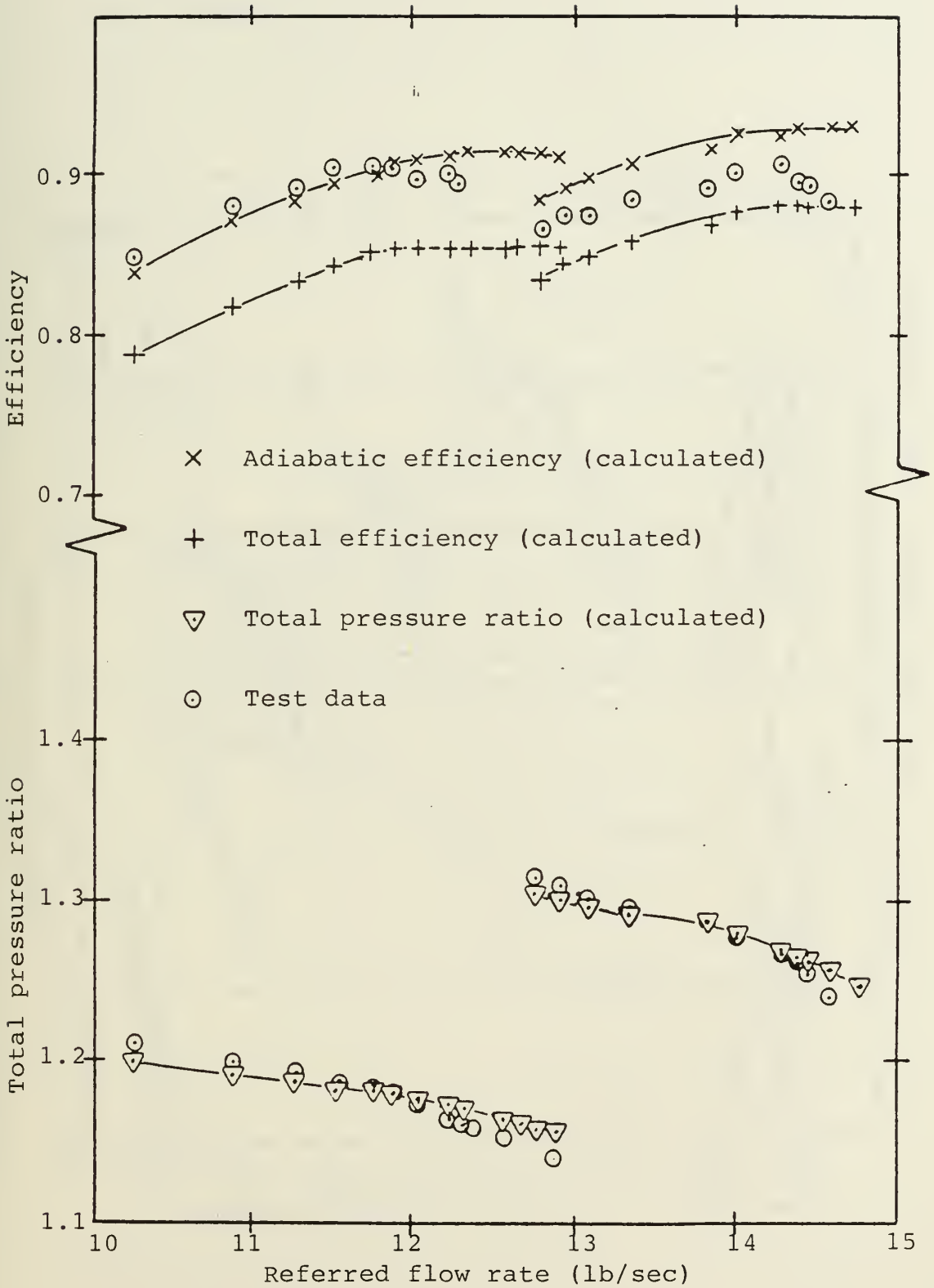

Figure 17. Calculated and measured compressor performance maps at 60% and 70% design speed.

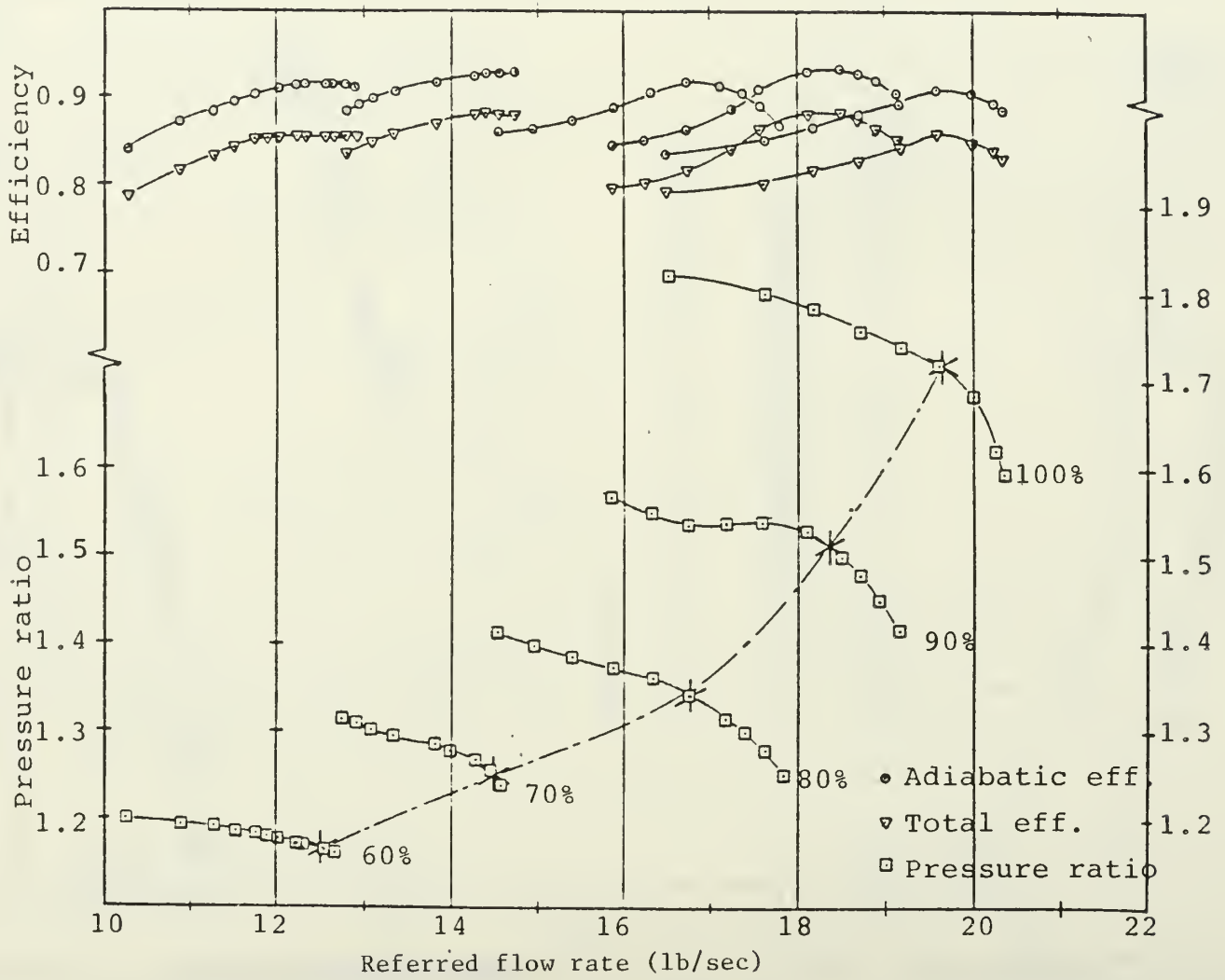

Figure 18. Calculated compressor performance map. (Broken line identifies peak efficiency conditions)

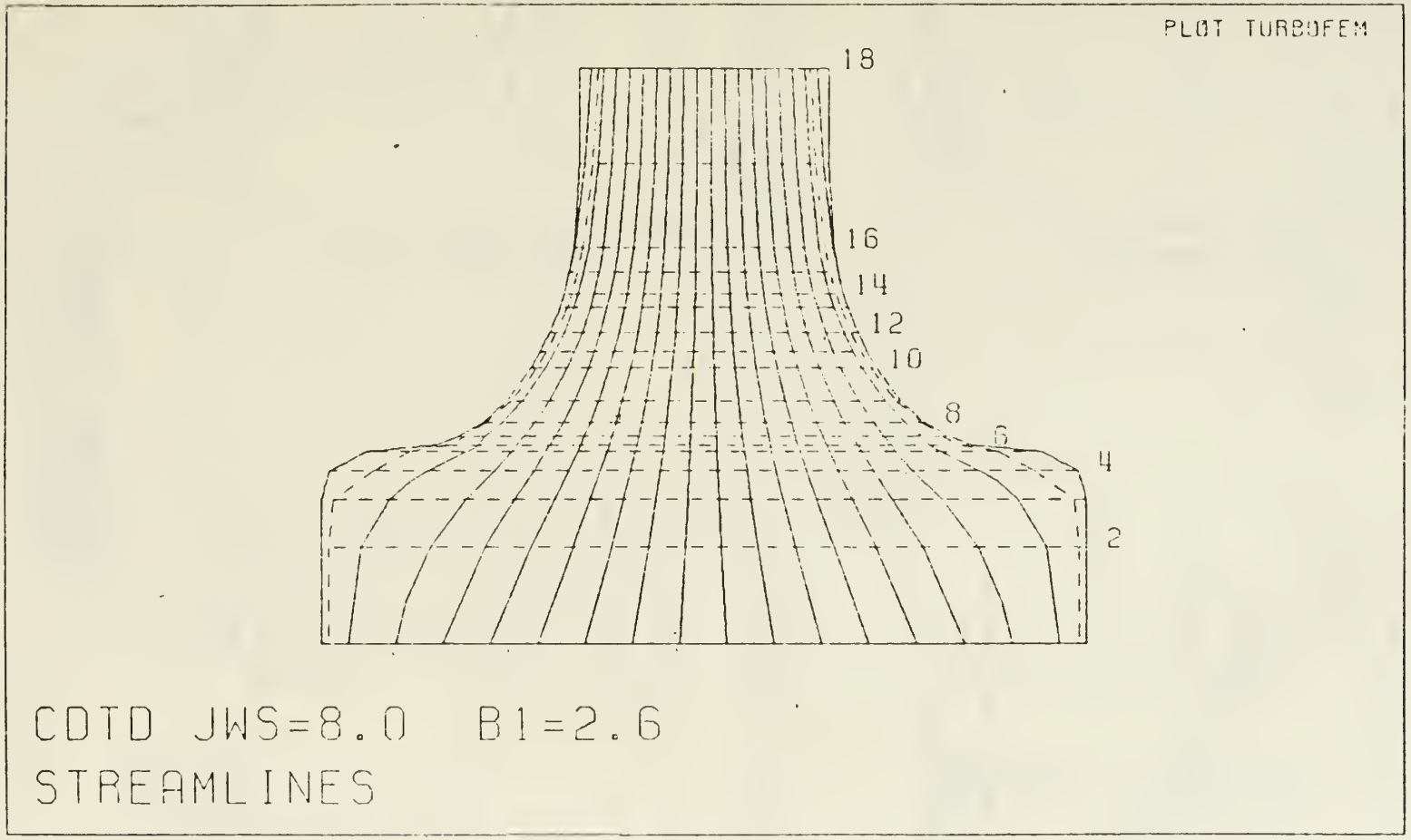

Figure 19. CDTD test section cross-section.

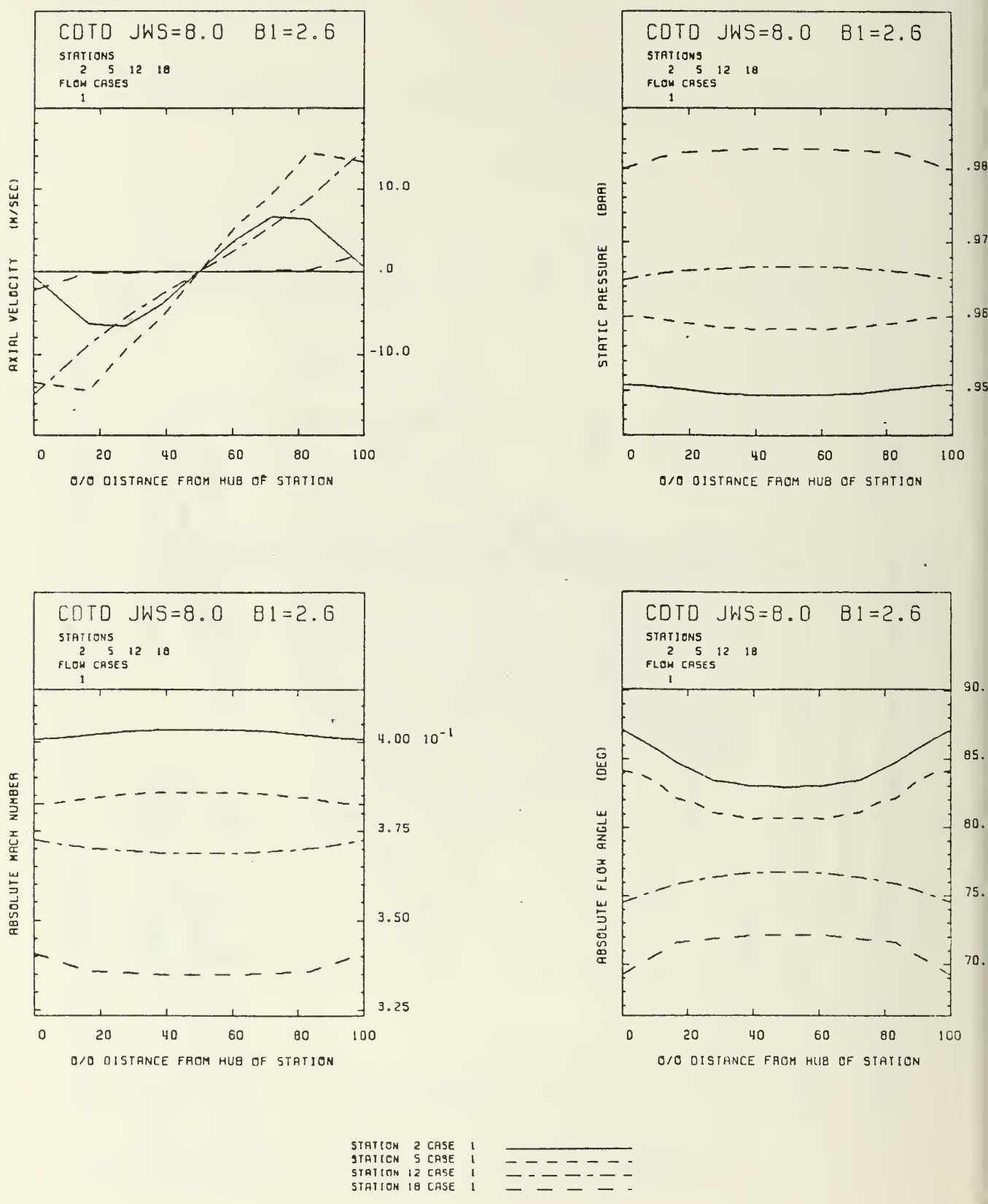

Figure 20. Spanwise distribution of flow properties as a function of flow station.

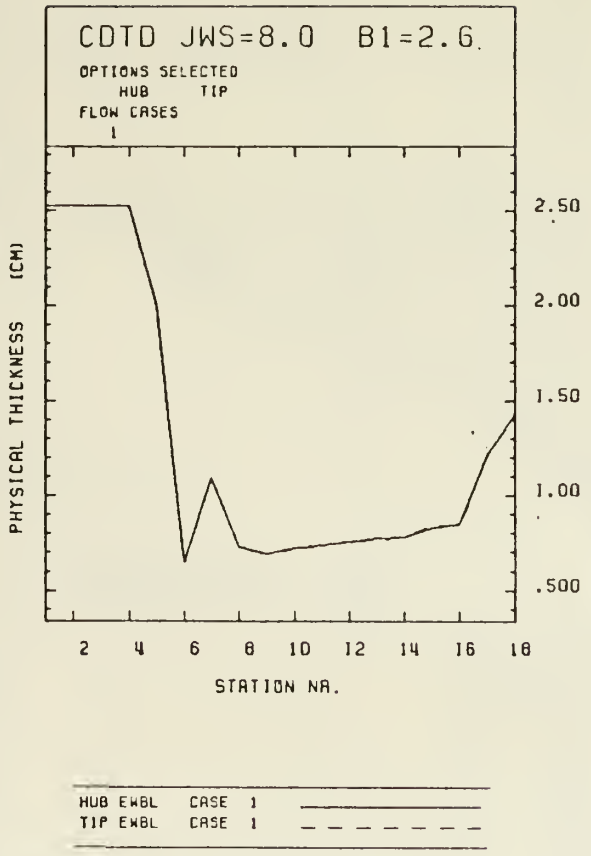

Figure 21. Boundary layer development as a function of flow station.

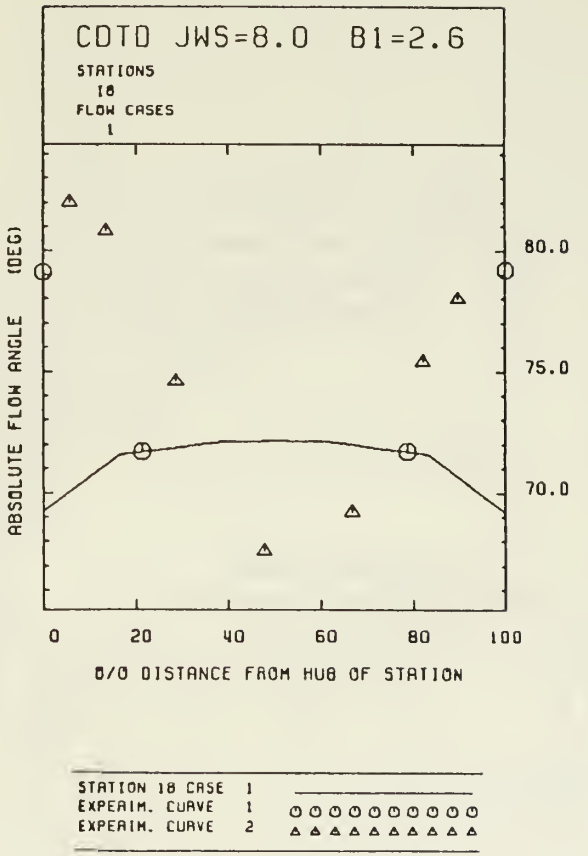

Figure 22. Comparison of predicted and measured flow angles.

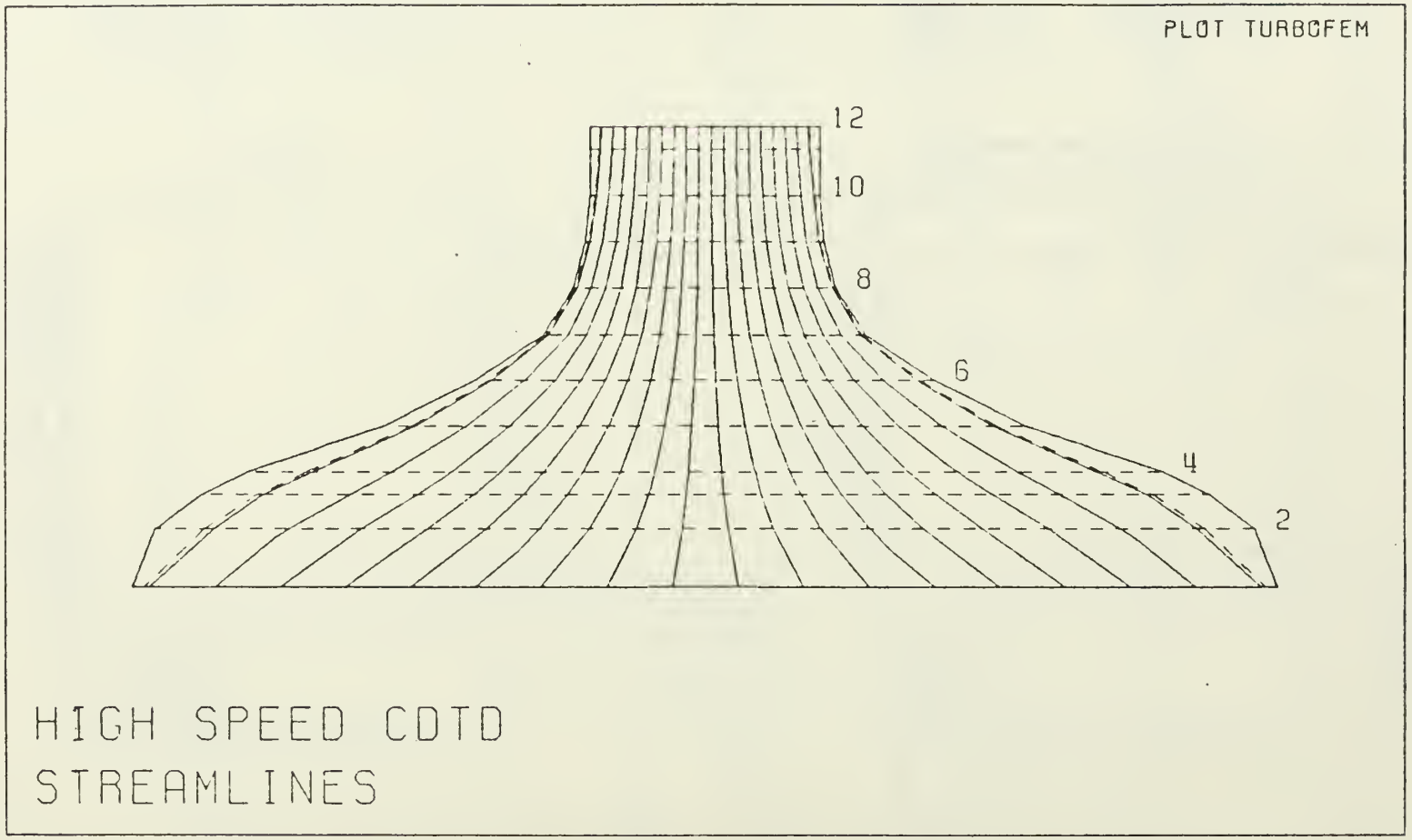

Figure 23. High speed CDTD streamlines.

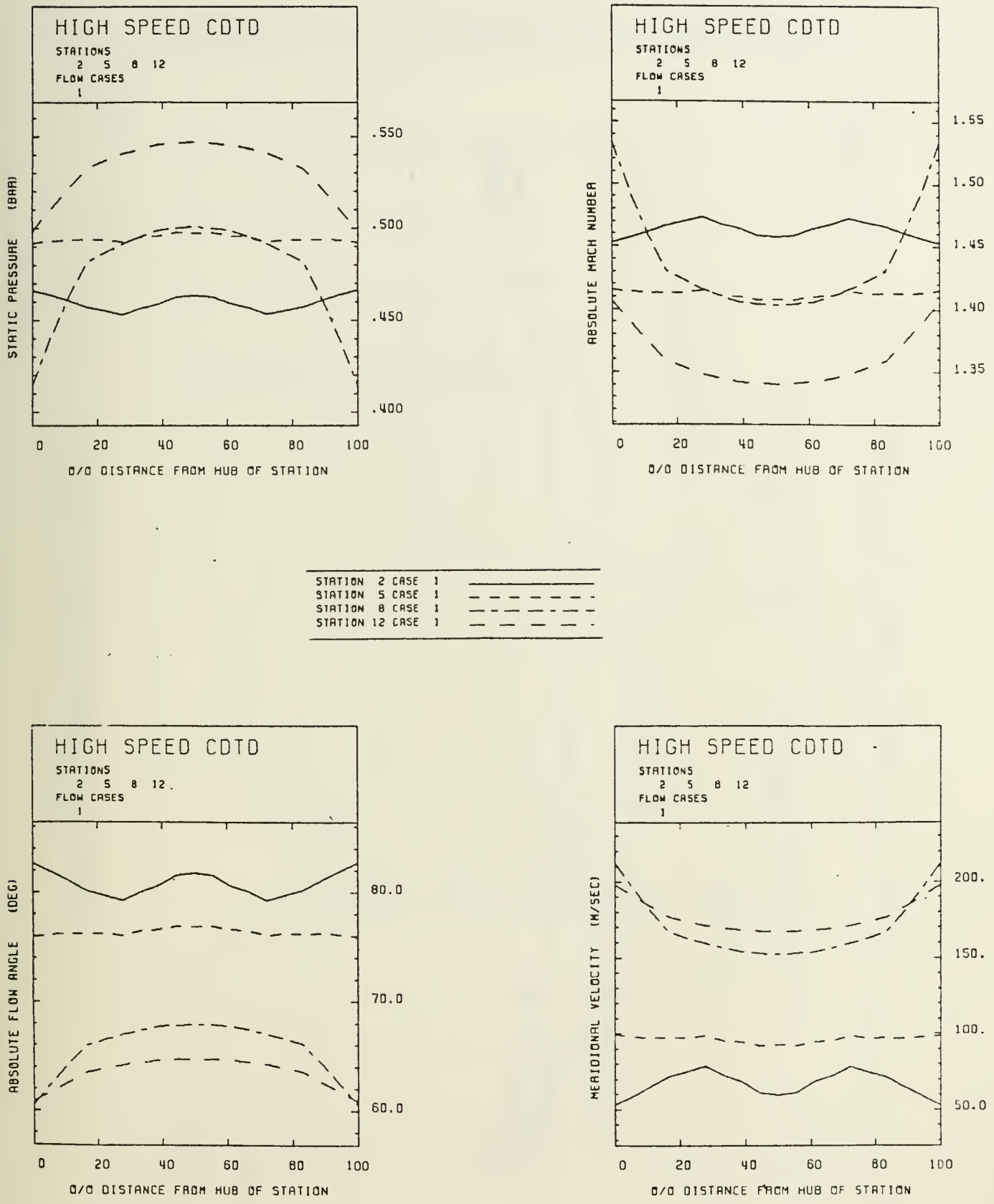

Figure 24. High speed CDTD flow properties.

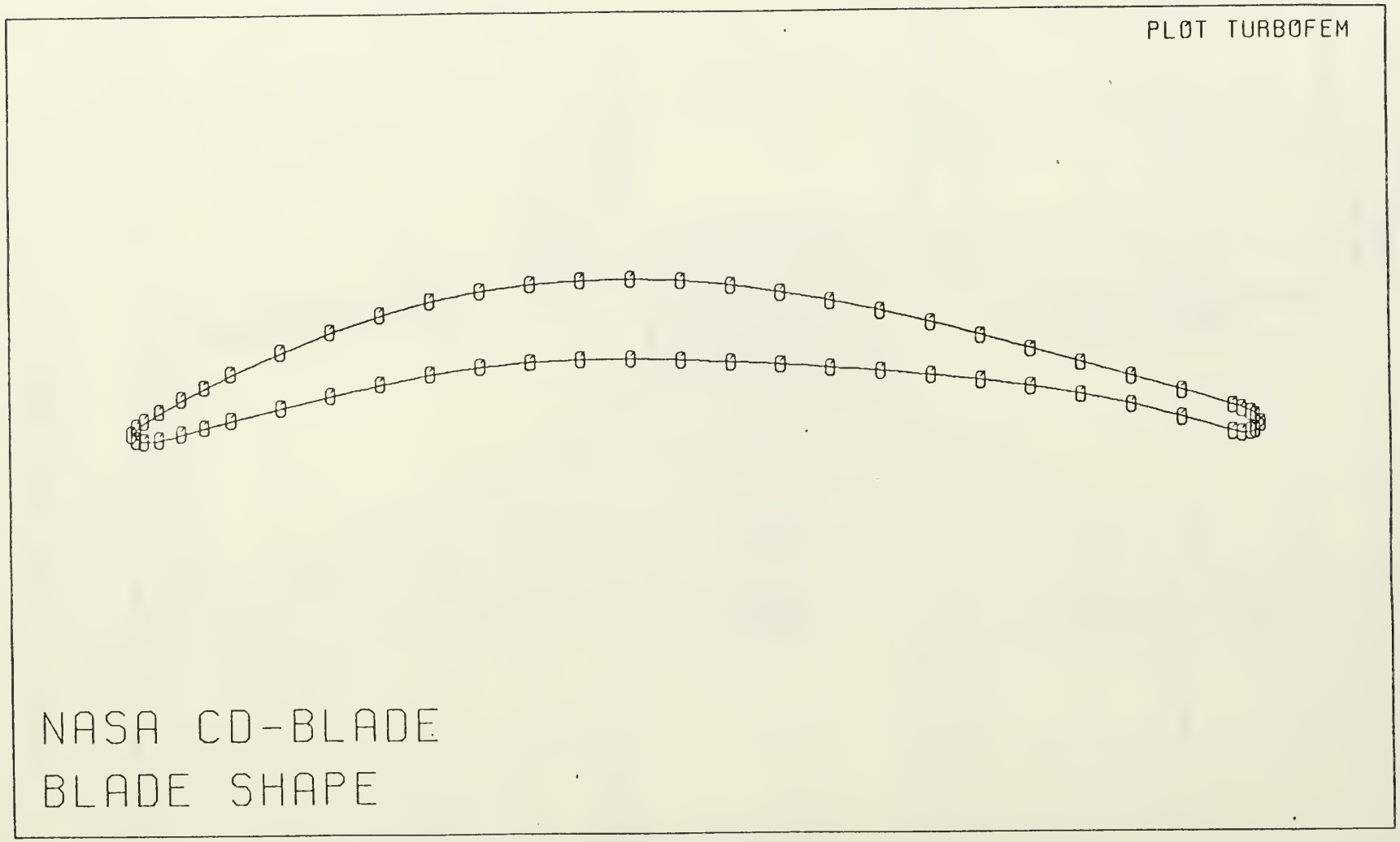

Figure 25. NASA CD blade profile.

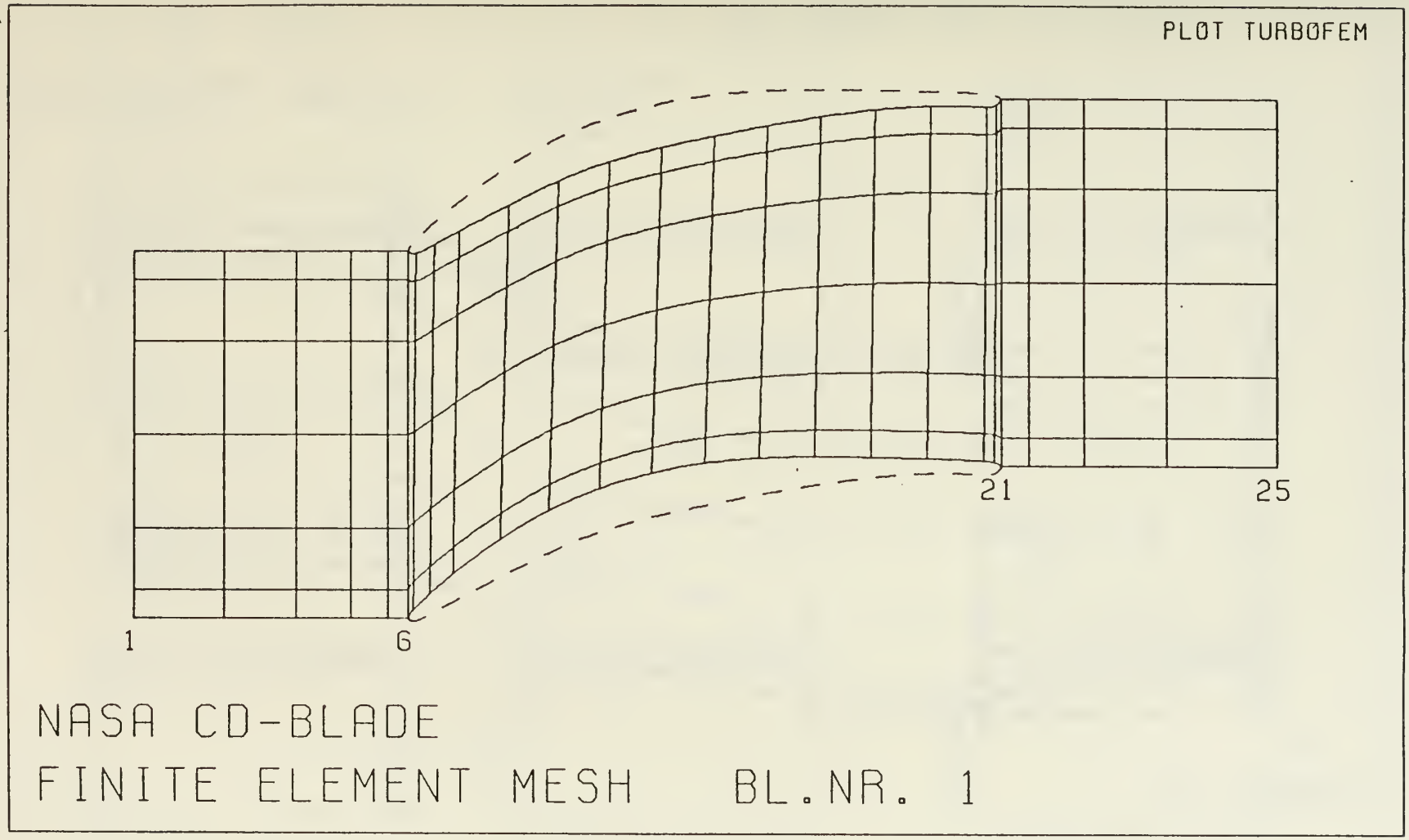

Figure 26. NASA CD blade finite element mesh.

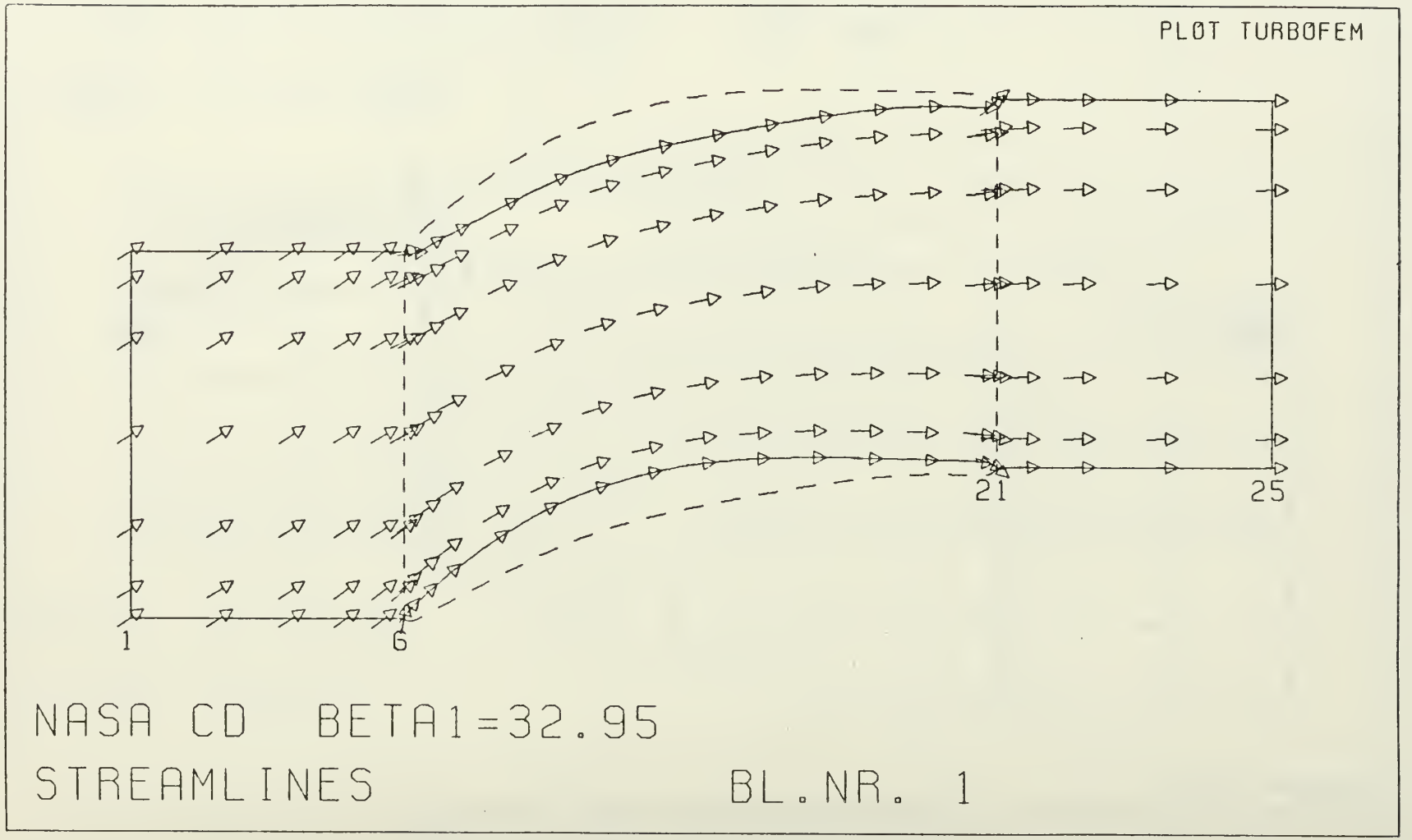

Figure 27. Plot of streamlines through the cascade.

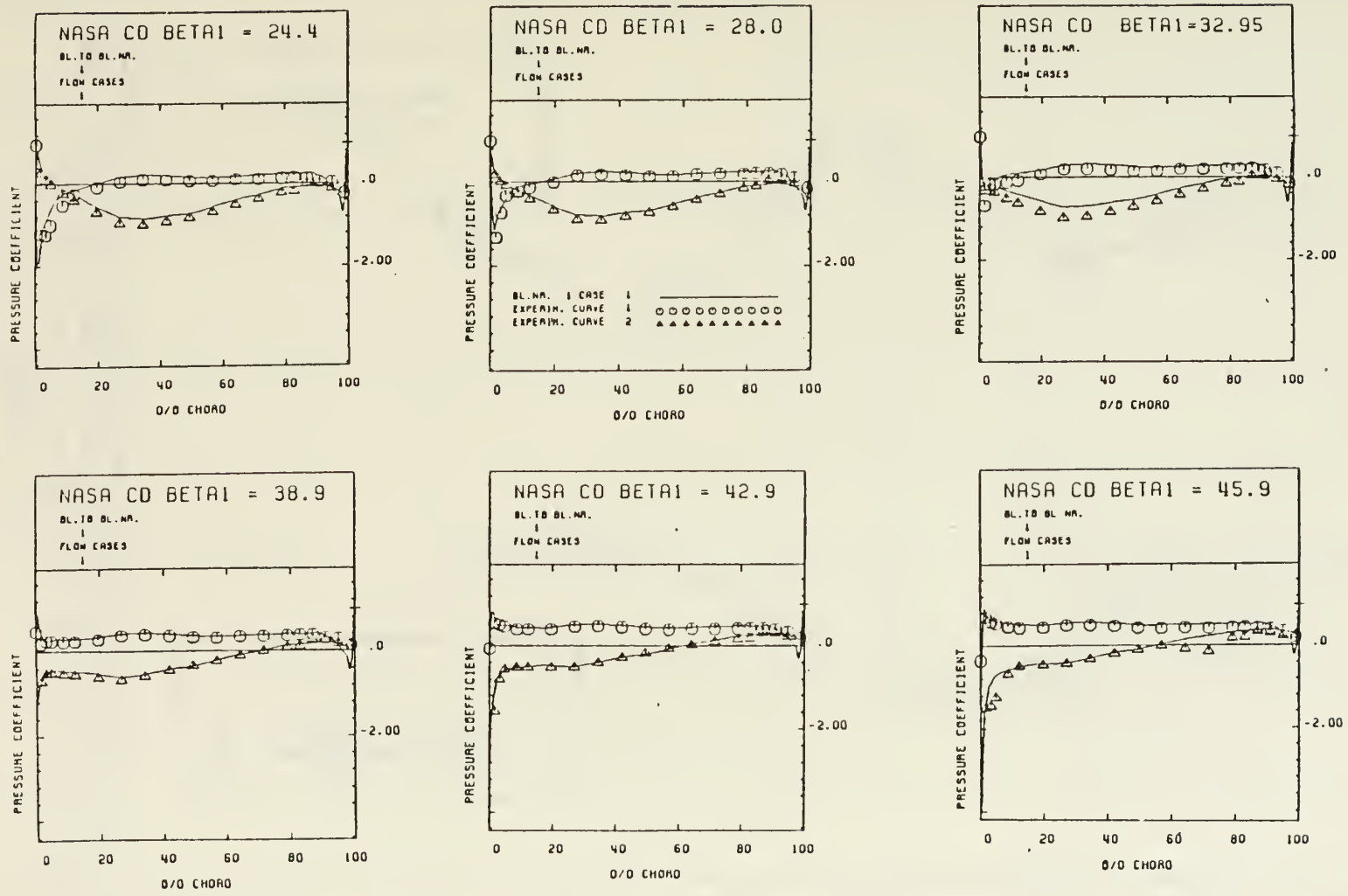

Figure 28. Predicted and measured surface pressures.

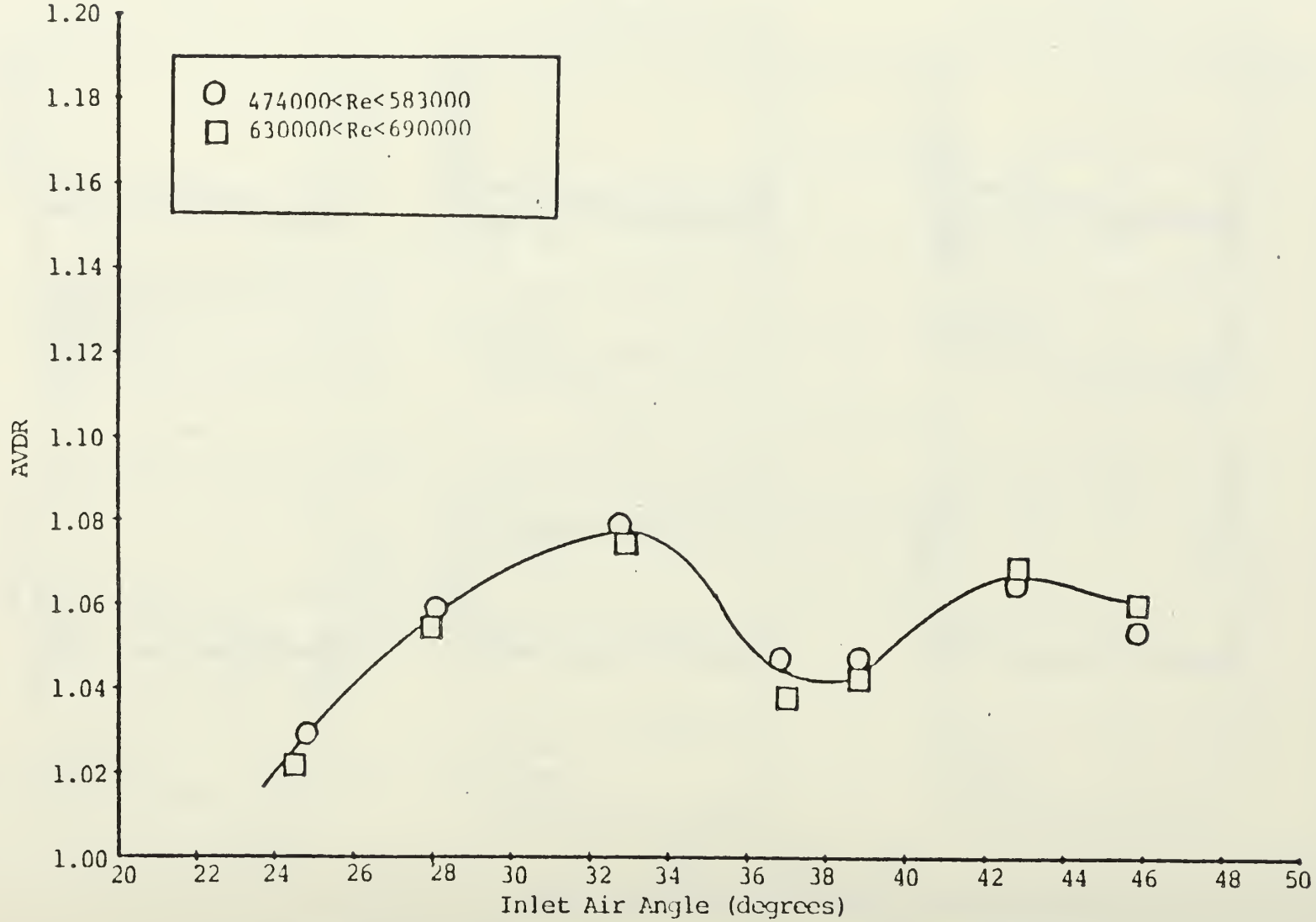

Figure 29. AVDR vs. air inlet angle.

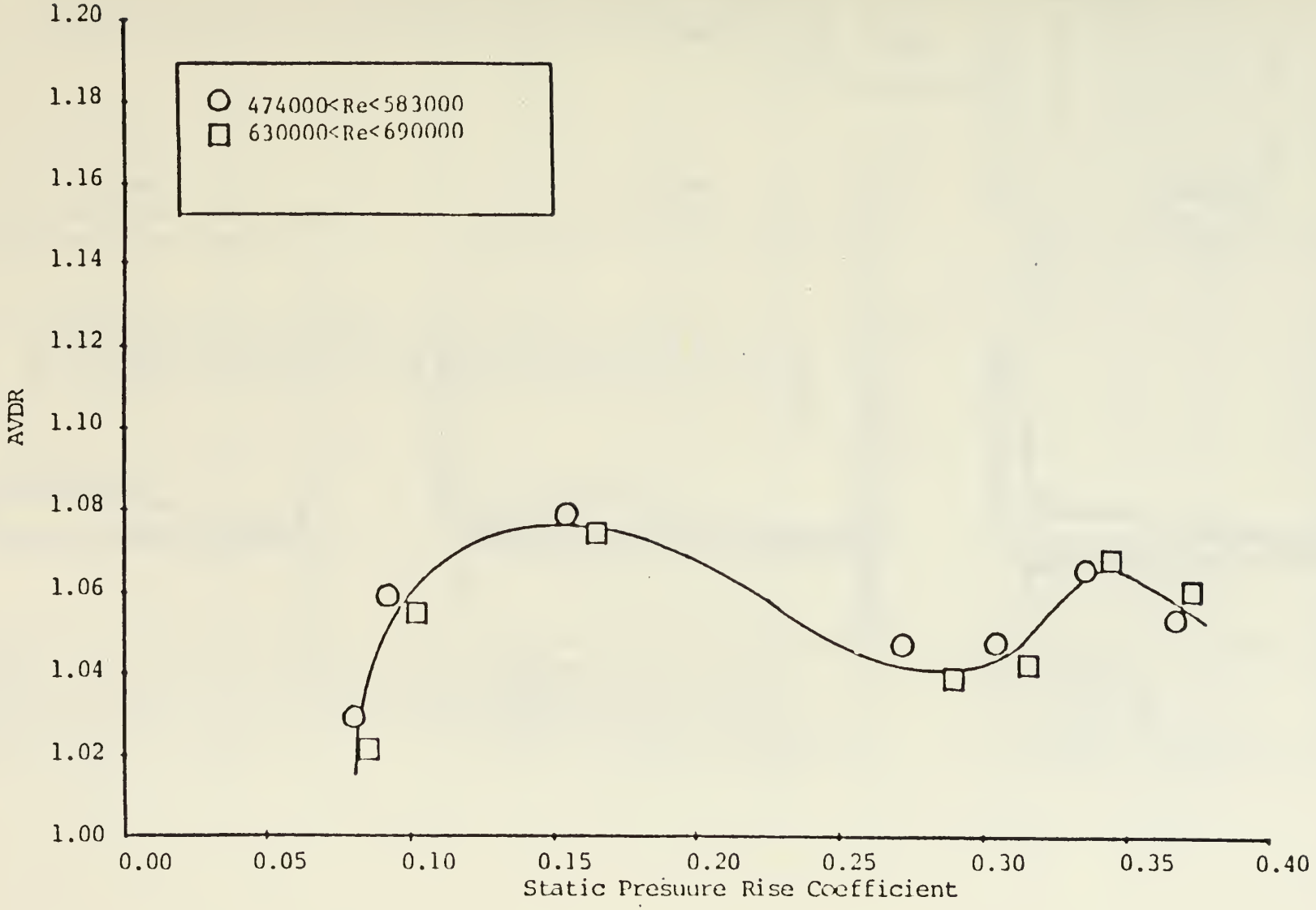

Figure 30. AVDR vs. static pressure rise coefficient

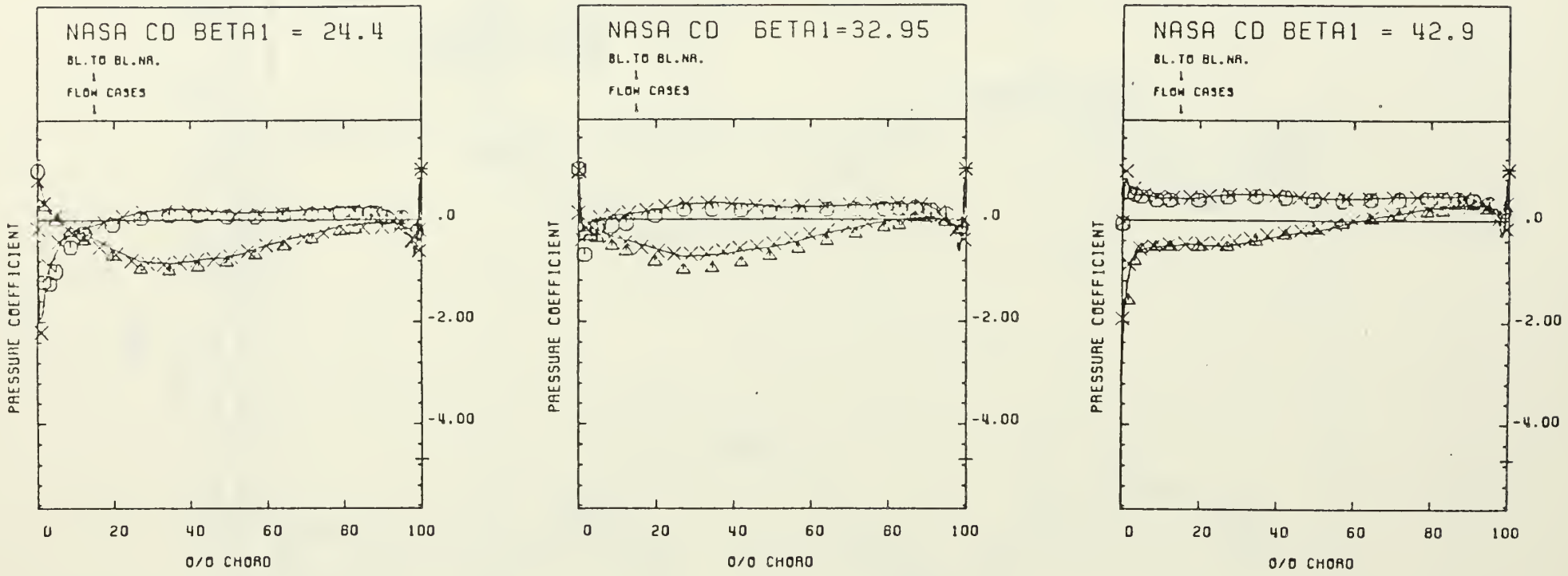

———— Q3DFLO-81

×××××××××× QSONIC

oooooooooo TEST DATA (PRESSURE SIDE)

▲▲▲▲▲▲▲▲▲▲ TEST DATA (SUCTION SIDE)

Figure 31. Comparison of Q3DFLO-81 and QSONIC.

TABLE I - CD COMPRESSOR CASCADE PARAMETERS

Blade type	CD
Number of blades	20
Spacing (inches)	3.0
Solidity	1.67
Thickness (% chord)	7.0
Stagger angle	14.27

TABLE II - CD BLADE COORDINATES

X-COORD.	Y-PRESS.	Y-SUCT.
0.0	0.045	0.045
0.022	-----	0.084
0.057	0.002	-----
0.222	0.044	0.196
0.444	0.101	0.307
0.666	0.155	0.403
0.888	0.207	0.488
1.110	0.255	0.561
1.332	0.299	0.621
1.554	0.330	0.663
1.776	0.350	0.691
1.998	0.359	0.705
2.220	0.359	0.708
2.442	0.352	0.701
2.664	0.342	0.681
2.886	0.331	0.650
3.108	0.317	0.610
3.330	0.301	0.563
3.552	0.281	0.510
3.774	0.257	0.453
3.996	0.227	0.393
4.218	0.191	0.332
4.440	0.146	0.270
4.662	0.089	0.208
4.884	0.019	0.145
4.925	0.004	-----
4.964	-----	0.122
5.010	0.062	0.062

REFERENCES

1. Wu, C. H., "A General Theory of Three Dimensional Flow in Subsonic and Supersonic Turbomachines of Axial-Radial and Mixed Flow Type," NACA, TN 2604, 1952.

2. Hirsch, CH. and Warzee, G., "A Finite Element Method for Through Flow Calculations in Turbomachines," ASME Journal of Fluid Engineering, pp. 403-421, September 1976.

3. Hirsch, CH. and Warzee, G., "An Integral Quasi-3D Finite Element Calculation Program for Turbomachinery Flow," ASME Journal of Engineering for Power, Vol. 01, pp. 141-148, January 1979.

4. Schulz, H. D., "Guide to Using the Finite Element Code Q3DFLO-81 on the NPS IBM 370," Naval Postgraduate School, Turbopropulsion Laboratory Technical Note TPL-TN-84-01, June 1984.

5. Erwin, J. R., "A Review of the Design of the NPS/TPL Transonic Compressor," Contractor Report NPS67-83-004CR, Naval Postgraduate School, Monterey, CA, March 1983.

6. Erwin, J. R., Phillips, R., Schulz, H. D. and Shreeve, R. P., "Development of a Centrifugal Diffuser Test Device, Part I - Design and Construction of Low Speed Aparatus," Naval Postgraduate School Project Report, NPS67-84-003PR, September 1984.

7. Schulz, H. D. and Shreeve, R. P., "Development of a Centrifugal Diffuser Test Device, Part II - Initial Measurements and Flow Analysis," Naval Postgraduate School Project Report, NPS67-84-004PR, September 1984.

8. Sanger, N. L., "The Use of Optimization Techniques to Design Controlled Diffusion Compressor Blading," NASA Technical Memorandum 82763, Lewis Research Center, Cleveland, Ohio, 1982.

9. Rose, C. C. and Guttormson, D. L., "Installation and Test of a Rectilinear Cascade," Master's Thesis, Naval Postgraduate School, Monterey, California, 1964.

10. Koyuncu, Y, "Report of Tests of a Compressor Configuration of CD Blading," Master's Thesis, Naval Postgraduate School, Monterey, California, 1984.

11. Himes, S. J., "Report of Tests of a Compressor Configuration of DCA Blading," Master's Thesis, Naval Postgraduate School, Monterey, California, 1983.

REFERENCES

12. Farrell, Ch., "Quasi-3D Full Potential Transonic Blade-to-Blade-Code," NASA Hand out, Draft of Technical Paper, Conference on Turbomachinery Flow Analysis Methods--A Status Report on Maturing Codes, Conference at NASA Lewis Research Center, 14-15 October 1981.

13. Molloy, Jr., W. D., "Preliminary Measurements and Code Calculations of Flow Through a Cascade of DCA Blading at a Solidity of 1.67," Master's Thesis, Naval Postgraduate School, Monterey, California, 1982.

INITIAL DISTRIBUTION LIST

1. Commander
   Naval Air Systems Command
   Washington, DC 20361
   Attention: Code AIR 310 — 1
   Code AIR 310E — 1
   Code AIR 320D — 1
   Code AIR 530 — 1
   Code AIR 536 — 1
   Code AIR 00D — 14
   Code AIR 03D — 1

2. Office of Naval Research
   800 N. Quincy Street
   Arlington, VA 22217
   Attention: Dr. A. D. Wood — 1
   Dr. M. K. Ellingsworth — 1

3. Commanding Officer
   Naval Air Propulsion Center
   Trenton, NJ 08628
   Attention: G. Mangano, PE-31 — 1

4. Commanding Officer — 1
   Naval Air Development Center
   Warminster, PA 19112
   Attention: AVTD

5. Library — 1
   Army Aviation Material Laboratories
   Department of the Army
   Fort Eustis, VA 23604

6. Dr. Arthur J. Wennerstrom — 1
   AFWAL/POTX
   Wright-Patterson AFB
   Dayton, OH 45433

7. Air Force Office of Scientific Research — 1
   AFOSR/NA
   Bolling Air Force Base
   Washington, DC 20332
   Attention: Mr. James Wilson

8. National Aeronautics & Space Administration
   Lewis Research Center
   21000 Brookpark Road
   Cleveland, OH 44135
   Attention: Chief, Internal Fluid Mechanics Division 3
   Library 1

9. Library 1
   General Electric Company
   Aircraft Engine Technology Division
   DTO Mail Drop H43
   Cincinnati, OH 45215

10. Library 1
    Pratt & Whitney Aircraft Group
    Post Office Box 2691
    West Palm Beach, FL 33402

11. Library 1
    Pratt-Whitney Aircraft Group
    East Hartford, CT 06108

12. Library 1
    Curtis Wright Corporation
    Woodridge, NJ 07075

13. Library 1
    AVCO/Lycoming
    550 S. Main Street
    Stratford, CT 06497

14. Library 1
    Teledyne CAE, Turbine Engines
    1330 Laskey Road
    Toledo, OH 43612

15. Library 1
    Williams International
    P. O. Box 200
    Walled Lake, MI 48088

16. Library 1
    Detroit Diesel Allison Division G.M.C.
    P. O. Box 894
    Indianapolis, IN 46202

17. Library 1
    Garrett Turbine Engine Company
    111 S. 34th Street
    P. O. Box 5217
    Phoenix, AZ 85010

8. Professor J. P. Gostelow — 1
School of Mechanical Engineering
The New South Wales Institute of Technology
New South Wales
AUSTRALIA

19. Dr. G. J. Walker — 1
Civil and Mechanical Engineering
Department
The University of Tasmania
Box 252C
GPO Hobart, Tasmania 7110
AUSTRALIA

20. Professor F. A. E. Breugelmans — 1
Institut von Karman de la Dynamique
des Fluides
72 Chausee de Waterloo
1640 Rhode-St. Genese
BELGIUM

21. Professor Ch. Hirsch — 5
Vrije Universiteit Brussel
Pleinlaan 2
1050 Brussels
BELGIUM

22. Director — 1
Gas Turbine Establishment
P. O. Box 305
Jiangyou County
Sichuan Province
CHINA

23. Professor C. H. Wu — 1
P. O. Box 2706
Beijing 100080
CHINA

24. Director, Whittle Laboratory — 1
Department of Engineering
Cambridge University
ENGLAND

25. Professor Jacques Chauvin — 1
Universite d'Aix-Marseille
1 Rue Honnorat
Marseille
FRANCE

26. Mr. Jean Fabri — 1
ONERA
29, Ave. de la Division Leclerc
92 Chatillon
FRANCE

27. Professor D. Adler — 1
Technion Israel Institute of Technology
Department of Mechanical Engineering
Haifa 32000
ISRAEL

28. Dr. P. A. Paranjpe — 1
Head, Propulsion Division
National Aeronautics Laboratory
Post Bag 1700
Bangalore - 17
INDIA

29. Dr. W. Schlachter — 1
Brown, Boveri Company Ltd.
Dept. T-T
P. O. Box CH-5401 Baden
SWITZERLAND

30. Professor Leonhard Fottner — 1
Department of Aeronautics and Astronautics
German Armed Forces University
Hochschule des Bundeswehr
Werner Heisenbergweg 39
8014 Neubiberg near Munich
WEST GERMANY

31. Professor Dr. Ing. Heinz E. Gallus — 1
Lehrstuhl und Institut feur Strahlantiebe
und Turbourbeitsmashinen
Rhein.-Westf. Techn. Hochschule Aachen
Templergraben 55
5100 Aachen
WEST GERMANY

32. Dr. Ing. Hans-J. Heinemann — 1
DFVLR-AVA
Bunsenstrasse 10
3400 Geottingen
WEST GERMANY

33. Dr. H. Weyer — 1
DFVLR
Linder Hohe
505 Porz-Wahn
WEST GERMANY

34. Dr. Robert P. Dring — 1
United Technologies Research Center
East Hartford, CT 06108

35. Chairman — 1
Aeronautics and Astronautics Department
31-265 Massachusetts Institute of Technology
Cambridge, Massachusetts 02139

36. Dr. B. Lakshminarayana — 1
Professor of Aerospace Engineering
The Pennsylvania State University
233 Hammond Building
University Park, Pennsylvania 16802

37. Mr. R. A. Langworthy — 1
Army Aviation Material Laboratories
Department of the Army
Fort Eustis, VA 23604

38. Professor Gordon C. Oates — 1
Department of Aeronautics and Astronautics
University of Washington
Seattle, Washington 98105

39. Mechanical Engineering Department
Virginia Polytechnic Institute and
State University
Blacksburg, VA 24061
Attn: Professor W. O'Brian — 1
Professor H. Moses — 1

40. Professor T. H. Okiishi — 1
Professor of Mechanical Engineering
208 Mechanical Engineering Building
Iowa State University
Ames, Iowa 50011

41. Dr. Fernando Sisto — 1
Professor and Head of Mechanical
Engineering Department
Stevens Institute of Technology
Castle Point
Hoboken, NJ 07030

42. Dr. Leroy H. Smith, Jr. — 1
Manager, Compressor and Fan
Technology Operation
General Electric Company
Aircraft Engine Technology Division
DTO Mail Drop H43
Cincinnati, OH 45215

43. Dr. W. Tabakoff — 1
Professor, Department of Aerospace Engineering
University of Cincinnati
Cincinnati, OH 45221

44. Mr. P. Tramm — 1
Manager, Research Labs
Detroit Diesel Allison Division
Genteral Motors
P. O. Box 894
Indianapolis, IN 46206

45. Mr. P. F. Yaggy — 1
Director
U. S. Army Aeronautical Research Laboratory
AMES Research Center
Moffett Field, CA 94035

46. Library — 2
Code 1424
Naval Postgraduate School
Monterey, CA 93943

47. Office of Research Administration — 1
Code 012
Naval Postgraduate School
Monterey, CA 93943

48. Defense Technical Information Center — 2
Cameron Station
Alexandria, VA 22314

49. Naval Postgraduate School
Monterey, CA 93943
Attn: Professor M. F. Platzer (67PL) — 1
Turbopropulsion Laboratory (67Sf) — 20